Modeling the response of a tumor-suppressive network to mitogenic and oncogenic signals

Xinyu Tian[a,b,c,1], Bo Huang[a,b,c,1], Xiao-Peng Zhang[d], Mingyang Lu[e], Feng Liu[a,b,c,2], José N. Onuchic[f,g,h,i,2], and Wei Wang[a,b,c,2]

[a]National Laboratory of Solid State Microstructures, Nanjing University, Nanjing 210093, China; [b]Department of Physics, Nanjing University, Nanjing 210093, China; [c]Collaborative Innovation Center of Advanced Microstructures, Nanjing University, Nanjing 210093, China; [d]Kuang Yaming Honors School, Nanjing University, Nanjing 210023, China; [e]The Jackson Laboratory, Bar Harbor, ME 04609; [f]Center for Theoretical Biological Physics, Rice University, Houston, TX 77005; [g]Department of Physics and Astronomy, Rice University, Houston, TX 77005; [h]Department of Chemistry, Rice University, Houston, TX 77005; and [i]Department of Biosciences, Rice University, Houston, TX 77005

Contributed by José N. Onuchic, April 19, 2017 (sent for review February 13, 2017; reviewed by Masaki Sasai and Jin Wang)

Intrinsic tumor-suppressive mechanisms protect normal cells against aberrant proliferation. Although cellular signaling pathways engaged in tumor repression have been largely identified, how they are orchestrated to fulfill their function still remains elusive. Here, we built a tumor-suppressive network model composed of three modules responsible for the regulation of cell proliferation, activation of p53, and induction of apoptosis. Numerical simulations show a rich repertoire of network dynamics when normal cells are subject to serum stimulation and adenovirus E1A overexpression. We showed that oncogenic signaling induces ARF and that ARF further promotes p53 activation to inhibit proliferation. Mitogenic signaling activates E2F activators and promotes Akt activation. p53 and E2F1 cooperate to induce apoptosis, whereas Akt phosphorylates p21 to repress caspase activation. These prosurvival and proapoptotic signals compete to dictate the cell fate of proliferation, cell-cycle arrest, or apoptosis. The cellular outcome is also impacted by the kinetic mode (ultrasensitivity or bistability) of p53. When cells are exposed to serum deprivation and recovery under fixed E1A, the shortest starvation time required for apoptosis induction depends on the terminal serum concentration, which was interpreted in terms of the dynamics of caspase-3 activation and cytochrome *c* release. We discovered that caspase-3 can be maintained active at high serum concentrations and that E1A overexpression sensitizes serum-starved cells to apoptosis. This work elucidates the roles of tumor repressors and prosurvival factors in tumor repression based on a dynamic network analysis and provides a framework for quantitatively exploring tumor-suppressive mechanisms.

cell-fate determination | oncogene activation | signal transduction

Keeping cell proliferation in check is essential for tumor suppression (1). Although the activation of oncogenes tends to induce cell transformation, a variety of innate mechanisms are engaged to protect against neoplastic progression by triggering cell-cycle arrest, senescence, or apoptosis while retaining the proliferative capacity of normal cells (2). Dysfunction of these mechanisms usually promotes tumorigenesis. Tumor repression is achieved via concerted actions of sensors, transducers, modulators, and effectors, which constitute a tumor-suppressive network. This complex network is interconnected to the machinery responsible for cell-cycle arrest and apoptosis. Although the operating mechanism of tumor suppression is a focus of intensive research (2), unraveling it has been a challenge.

As a tumor sensor, ARF is induced by activated oncogenes such as Myc and E1A (3). ARF transduces oncogenic signals by stabilizing and activating p53 (4). p53 is a potent tumor suppressor capable of inducing cell-cycle arrest, senescence, and apoptosis (5). Contrary to the ARF–p53 axis, environmental trophic factors such as growth factors and cytokines tend to trigger intracellular programs that buffer or repress proapoptotic signals. They do so mainly by activating receptor tyrosine kinases and signaling through the Ras/PI3K cascade, in which the Akt kinase acts as a key mediator and promotes cell survival (2, 6). On the other hand, the E2F family regulates the entry into and progression through the S phase of the cell cycle. Specifically, deregulated E2F1 promotes both cell proliferation and apoptosis (7).

Generally, the cell-fate decision depends on the competition between proapoptotic signals induced by tumor suppressors and prosurvival signals evoked by trophic factors. Consistent with this notion, cells exposed to oncogene activation are more susceptible to apoptosis upon serum withdrawal than in serum-rich situations (8–11). Despite this qualitative understanding, we still need a quantitative and comprehensive characterization of how cells respond to these competing signals.

Here, we construct a three-module network model to unravel the mechanism of tumor suppression following E1A activation. The modules detect and process physiological and oncogenic stimuli for cellular decision-making. We explore how cell fate is controlled by competing factors under various conditions and examine the impact of growth factors on apoptosis induction after serum starvation. Simulation results agree well with multiple experimental observations, and testable predictions are presented. This work provides an insight into how different signaling pathways are orchestrated dynamically to repress aberrant proliferation.

Significance

Mammalian cells have evolved to develop multiple mechanisms for tumor suppression. It remains challenging to dissect the dynamic mechanism by which signaling proteins are engaged in inhibiting aberrant cell proliferation. Here, we propose a comprehensive network model composed of three signaling pathways and show how this network responds to mitogenic and oncogenic signals. This modeling approach elucidates how a precise temporal control of signaling pathways modulates the cellular response. We reveal the underlying principle for cell-fate decision and identify the roles of the different network components in tumor inhibition. This study sheds light on how the tumor-suppressive function can be modulated by the dynamics of the signaling proteins.

Author contributions: X.-P.Z., F.L., J.N.O., and W.W. designed research; X.T. and B.H. performed research; F.L., J.N.O., and W.W. contributed new reagents/analytic tools; X.T., B.H., X.-P.Z., M.L., F.L., and W.W. analyzed data; and X.T., M.L., F.L., J.N.O., and W.W. wrote the paper.

Reviewers: M.S., Nagoya University; and J.W., Stony Brook University.

The authors declare no conflict of interest.

Freely available online through the PNAS open access option.

[1]X.T. and B.H. contributed equally to this work.

[2]To whom correspondence may be addressed. Email: jonuchic@rice.edu, fliu@nju.edu.cn, or wangwei@nju.edu.cn.

This article contains supporting information online at www.pnas.org/lookup/suppl/doi:10.1073/pnas.1702412114/-/DCSupplemental.

Models and Methods

The network model characterizes the cellular response to both growth factors and oncogenic signals derived from the overexpression of adenovirus E1A. Growth factors stimulate two pathways that separately promote cell proliferation and survival (Fig. 1*A*); E2F and Akt are the main regulators, respectively. Oncogenic signals not only promote cell proliferation but also activate the tumor-suppressive program that is mainly mediated by p53. Consequently, normal cells may undergo proliferation, cell-cycle arrest, or apoptosis. To dissect the dynamics and function of the network, we divided it into three functional modules (Fig. 1*B*). Notably, these modules are endowed with positive feedback loops, and thus some components exhibit switch-like behaviors when activated. Detailed descriptions of these modules are available in *SI Appendix*, *Methods* (see also *SI Appendix*, Fig. S1).

The framework of the module regulating cell proliferation is derived from ref. 12, with the incorporation of recent advances and the characterization of more interactions and processes (see *SI Appendix*, *Method S1*, for details). As the central node, E2F activators (E2F1, E2F2, and E2F3A; hereafter referred to as "E2F" for simplicity) are normally regulated by four positive feedback loops, i.e., E2F–cyclin E/Cdk2–RB, E2F–Myc, E2F–Myc–cyclin D/Cdk4/6–RB, and E2F self-activation. E1A can disrupt the delicate regulation of E2F by inactivating RB, resulting in ectopic expression of E2F and ARF induction (13, 14). E2F1 is distinguished from E2F2 and E2F3A because of their different functions and interactions with RB and E1A.

Two opposing factors affect the stability and activity of p53 via modulating MDM2. ARF forms a complex with MDM2 to inhibit its E3 ligase activity toward p53 (15), whereas growth factors not only facilitate the transcription of *mdm2* but also induce the activation of Akt (16). Activated Akt phosphorylates MDM2 to promote its nuclear accumulation and weaken its interaction with ARF (16–18). On the other hand, p53 induces the transcription of *mdm2* and *pten*, and PTEN dephosphorylates PIP3 to inhibit Akt activation (19, 20). Thus, the interactions between p53, PTEN, Akt, and MDM2 constitute a positive feedback loop (21).

The backbone of the apoptosis module is the caspase-activation cascade, which involves Bax activation, the release of cytochrome *c* (Cyt *c*) from mitochondria, apoptosome formation, and the activation of caspases (see *SI Appendix*, *Method S2*, for details). p53 initiates apoptosis by inducing Bax (22), which triggers the release of Cyt *c*, and E2F1 promotes apoptosis via inducing Apaf-1, procaspase-9, and procaspase-3 (23). Once in the cytosol, Cyt *c* binds to and activates Apaf-1, forming the apoptosome. Procaspase-9 forms dimers and becomes active; caspase-9 (Casp9), either free or bound to the apoptosome, leads to the conversion of procaspase-3 into caspase-3 (Casp3). The Casp3-mediated amplification loop of Cyt *c* release is responsible for switch-like activation of Casp3 (24). It was shown experimentally that a small pool of soluble Cyt *c* in the intermembrane space and Cyt *c* bound to the inner membrane of mitochondria are released sequentially during cell apoptosis (25, 26); this two-wave release of Cyt *c* is considered in the model. On the other hand, p53 induces p21, which promotes cell-cycle arrest and inhibits apoptosis. Akt-mediated phosphorylation of p21 enhances its accumulation in the cytosol. A mutual inhibition exists between Casp3 and p21: Cytosolic p21 can form a complex with procaspase-3, inhibiting its activation (27, 28), whereas Casp3 mediates the cleavage of p21 (29). Here, the persistent activation of Casp3 and p21 is taken as the indicator of apoptosis and cell-cycle arrest, respectively.

The concentration of each protein in the network, denoted by square brackets, is represented by a state variable. Their temporal evolution is governed by ordinary differential equations (ODEs) (*SI Appendix*, *Method S3*). The gene transcription mediated by transcription factors is characterized by the Hill function, whereas the (de)phosphorylation and (de)activation processes are taken as enzyme-catalyzed reactions and are assumed to follow the Michaelis–Menten kinetics (30–33). The definition of the variables and their initial concentrations, the description of reaction kinetics, and a set of standard parameter values are listed in *SI Appendix*, Tables S1–S3. The ODEs were numerically solved using MTALAB ode15s. The bifurcation diagrams were plotted using Oscill8.

Results

Differentiation Between Normal Mitogenic and Oncogenic Signals by ARF. E2F activators are well-known for the ability to govern the *R*-point in the cell cycle together with RB. It was shown that E2F

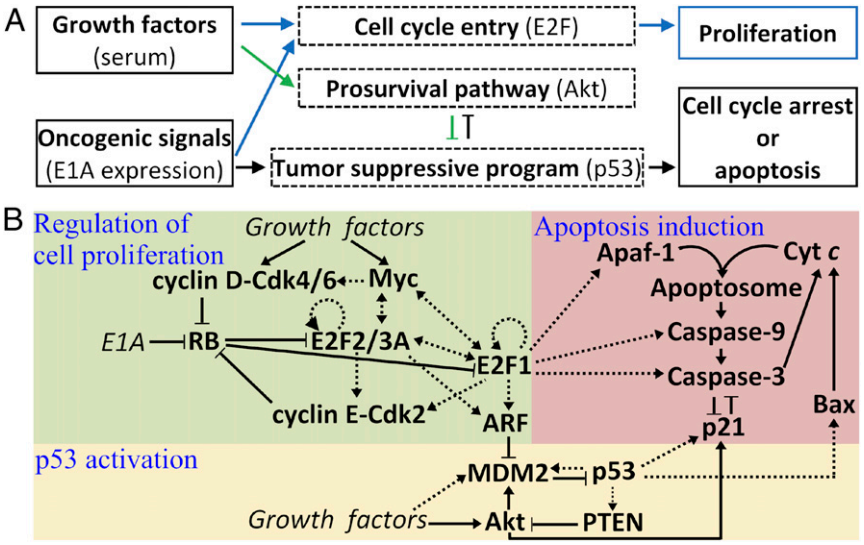

Fig. 1. A three-module model of the tumor-suppressive network. (*A*) Outline of the model. Growth factors stimulate two signaling pathways separately regulating cell-cycle progression and promoting cell survival. Oncogenic signals promote cell proliferation and activate tumor-suppressive programs via the canonical ARF–p53 axis. (*B*) The three-module network model characterizing the regulation of cell proliferation, p53 activation, and apoptosis induction. Dotted arrows, including two-way ones, represent transcriptional regulation; solid arrows and lines denote the promotion and inhibition, respectively, of production, transition, or activation.

behaves as a bistable switch in response to serum stimulation (12); this feature is reproduced here. A bistable regime exists in the bifurcation diagram of the steady-state level of E2F versus serum concentration (C), and the lower bifurcation point occurs at $C = 1\%$ (Fig. 2*A*). Of note, [E2F] equals the total concentration of all active forms of E2F. In contrast, the delicate R-point regulation is disrupted upon E1A expression; the steady-state E2F level rises toward saturation with increasing C. E1A induces ectopic expression of E2F even without serum. Consequently, ARF is actively induced by E2F, in contrast to its basal expression under normal growth conditions. This result agrees with the experimental observations that ARF becomes active only when the levels of its inducers exceed aberrantly high thresholds (14, 34, 35). Collectively, ARF is induced in an all-or-none manner to transduce oncogenic signals. The bifurcation diagrams for cyclin D and cyclin E are presented in *SI Appendix*, Fig. S2*A*.

Cyclin D is an early-response gene, reaching its steady level within 6 h after serum stimulation, whereas E2F becomes fully activated around 13 h (12); these features are recapitulated here (Fig. 2*B*). On the contrary, E1A alone fails to activate the production of cyclin D but induces high expression of E2F; as a consequence, the levels of cyclin E and ARF are markedly upregulated. The activation of E2F exhibits biphasic kinetics. Over the initial short period (0–5 h), [E2F] rises quickly (rapid phase); subsequently, it rises more slowly, and a long time is required for the saturation of [E2F] (slow phase). This biphasic feature is attributed mainly to the conversion of dominant regulators of E2F activity between the two phases: The rapid phase is triggered mainly by E1A-mediated RB suppression and E2F release, whereas the slow phase is associated with the transcriptional activity of E2F and E1A/RB-mediated inhibition of E2F degradation (see *SI Appendix*, Fig. S2 *B* and *C*, for details). Taken together, the dynamics of E2F and ARF expression differ remarkably between the two cases, so that normal signaling can be distinguished from aberrant proliferative signaling.

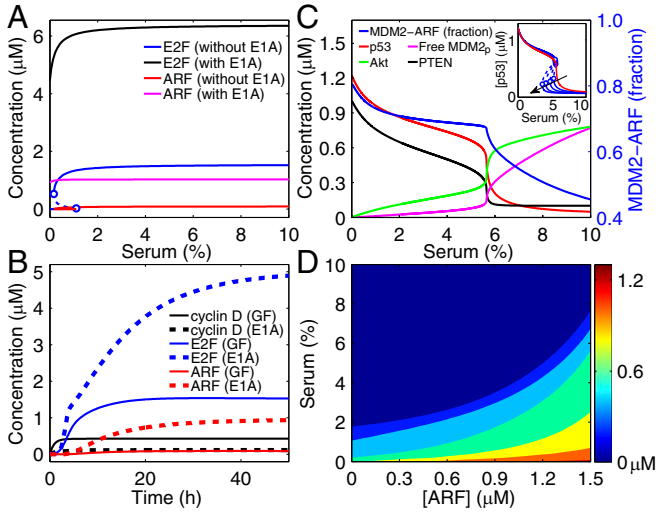

Fig. 2. Responses of activator E2F, ARF, and p53 to serum stimulation and E1A expression. (*A*) Bifurcation diagrams of the steady-state levels of E2F and ARF versus serum concentration with or without E1A expression. (*B*) Temporal evolution of the levels of cyclin D, E2F, and ARF in response to 10% serum (solid lines) or E1A expression with 0.1% serum (dashed lines). (*C*) Bifurcation diagrams for components in the p53 activation module with fixed E1A expression. The *Inset* shows the transition of the p53 kinetic mode from ultrasensitivity to bistability. Following the direction of the arrow, the rate constant and Michaelis constant for Akt dephosphorylation take the following values: k_{DP3}/K_{Akt} = 9.6/0.2, 8.8/0.16, 8.01/0.12, 7.17/0.08, and 6.51/0.05. (*D*) Steady-state p53 level as a function of independent serum and ARF concentrations. Here, [ARF] denotes the total amount of ARF, including free ARF, the MDM2–ARF (MA) and MDM2$_P$–ARF (M_PA) complexes. The dynamics of MA and M_PA obey *SI Appendix, Method 3*, Eqs. **S19** and **S20**, whereas [free ARF] = [ARF] − [MA] − [M_PA] replaces *SI Appendix, Method 3*, Eq. **S11 (b)**. The colored scale denotes the p53 level.

Dynamics of p53 Activation. p53 activation by ARF is essential to the initiation of tumor-suppressive programs. Because of the p53–PTEN–Akt–MDM2 positive feedback loop, the dependence of steady-state concentrations of these proteins on the serum concentration C can be ultrasensitive (Fig. 2*C*). The p53 level depends on C as follows: For $C \leq 5.5\%$ [p53] remains at relatively high levels (ON state), but it drops steeply to low levels (OFF state) around 6% and remains there thereafter. A similar transition mode has been reported previously (21, 36). The transition point is set around $C = 5.5\%$ to match the experimental observation that high levels of p53 can be induced when cells are supplied with 5% serum (37, 38) (Of note, this value is cell-type specific). Moreover, changing the feedback strength can switch the dependence of p53 levels on C from ultrasensitivity to bistability, with the upper bifurcation point changing slightly (Fig. 2*C*, *Inset*). Unless otherwise specified, p53 always operates in the ultrasensitive mode in the following analysis.

ARF and Akt are two opposing factors regulating p53 levels via MDM2. Unlike p53, the concentrations of free phosphorylated MDM2 (MDM2$_p$) and active Akt switch to relatively high levels after $C = 6\%$. Consistently, MDM2 in complex with ARF is the dominant form of MDM2 for $C < 6\%$, leading to the sequestration of MDM2 in the nucleolus and p53 activation; for $C > 6\%$, Akt phosphorylates MDM2 to promote its nuclear entry and weaken its interaction with ARF, resulting in MDM2$_p$ upregulation and p53 inactivation.

When both the concentrations of serum and ARF are controllable inputs, the steady-state level of p53 is represented by a contour map (Fig. 2*D*). Because growth factors facilitate both *mdm2* expression and the accumulation of MDM2$_p$ via Akt, Fig. 2*D* is significantly different from *SI Appendix*, Fig. S2*D*, which shows [p53] as a function of [ARF] and [Akt]. The contour map in Fig. 2*D* can be roughly divided into three regions: (*i*) the deep blue region represents the inactive state of p53, in which the impact of serum on p53 expression suppresses that of ARF; (*ii*) the light blue and green regions correspond to moderate levels of p53, with the effects of serum and ARF being comparable; and (*iii*) the yellow and red regions denote the highly active state of p53, in which the influence of ARF is predominant. Together, the p53 level depends on the relative strength of pro- versus antiproliferative signals.

Cell-Fate Determination Under Diverse Conditions. Activated p53 induces p21 and Bax, which inhibit and promote the activation of Casp3, respectively. With fixed E1A expression, the steady-state levels of p21 and Casp3 can exhibit bistability over a range of serum concentrations (Fig. 3*A*). Two saddle-node bifurcation points divide the serum concentration into three ranges: low (0–2%), intermediate (2–5.5%), and high (5.5–10%). Given that the initial concentrations of all species are their steady-state levels at 10% serum without E1A, the cell will sequentially undergo proliferation, cell-cycle arrest, and apoptosis when C is decreased from 10 to 0%.

At high serum levels, p53 remains inactive, and both free p21 and Bax are kept at low levels (*SI Appendix*, Fig. S3). Cyt *c* is maintained in mitochondria, and little apoptosome is formed. Thus, little Casp3 is produced despite the high expression of procaspase-3 by E2F1. Consequently, cell proliferation is permitted. At moderate serum levels, p21 and Bax are induced by p53; although Bax promotes Cyt *c* release, Akt-mediated phosphorylation of p21 enhances its localization in the cytosol to inhibit procaspase-3 activation. Thus, Casp3 is still at low levels, and cell-cycle arrest is

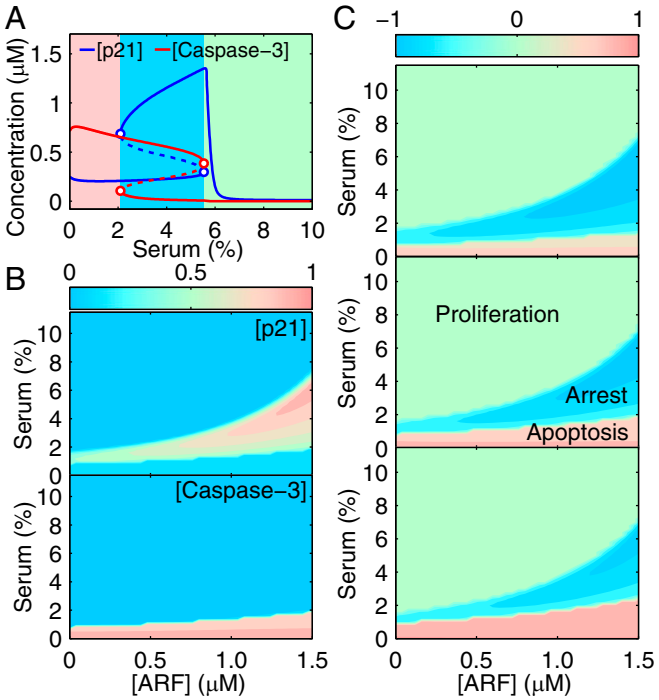

Fig. 3. Cell-fate decisions among proliferation, cell-cycle arrest, and apoptosis. (*A*) Steady-state levels of p21 (including phosphorylated and nonphosphorylated forms) and Casp3 versus serum concentration. (*B*) Dependence of the steady-state levels of p21 and Casp3 on independent ARF and serum concentrations. Protein levels are normalized by their respective maxima and are shown in contour maps. (*C*) Distribution of cell fates. By subtracting [p21] from [Casp3] in *B*, we roughly depict the distribution of cell fates. Compared with those in the middle panel, the E2F1-dependent expression rates of Apaf1, procaspase-9, and procaspase-3 drop (in the top panel) or rise (in the bottom panel) by 12.5%. The notation for [ARF] is the same as in Fig. 2*D*.

induced. Conversely, p21 phosphorylation becomes weak at low serum levels, and Casp3 is activated to trigger apoptosis.

More generally, the steady-state levels of p21 and Casp3 are calculated when the concentrations of both serum and ARF are independent inputs (Fig. 3*B*). Because p21 and Casp3 antagonize each other, they either are predominant in different regions or are simultaneously inactive. By subtracting the p21 level from the Casp3 level (both levels normalized by their respective maxima), we got a new plot reflecting the distribution of three cell fates (Fig. 3*C*, *Middle*). The comparison between Figs. 2*D* and 3*C* reveals that activated p53 inhibits cell proliferation, whereas the relative strength of prodeath versus antideath signals guides the decision between cell-cycle arrest and apoptosis.

The distribution of cell fates is also affected by E2F1 activity, p21/Casp3 interaction, and the kinetic mode of p53. First, increasing the transcriptional rates of Apaf-1, procaspase-9, and procaspase-3 by E2F1 results in the expansion of the region corresponding to apoptosis (compare the three panels in Fig. 3*C*). This effect agrees with the notion that E2F1 contributes to p53-dependent apoptosis under oncogenic conditions (7, 39). This role is highlighted when cellular responses to E1A expression and to ARF overexpression alone are compared. Without E1A, overexpression of ARF facilitates cell-cycle arrest rather than apoptosis in the presence of serum stimulation (*SI Appendix*, Fig. S4*A*), in agreement with experimental observations (40, 41). Second, as the rate constant for forming the $p21_P$/procaspase-3 complex rises, the region corresponding to apoptosis shrinks (*SI Appendix*, Fig. S4*B*), indicating the antiapoptotic role of p21. Third, if the kinetic mode of p53 changes from ultrasensitivity to bistability, and the bistable regime enlarges, the right-side OFF-to-ON transition point of p21, which is governed by p53, moves leftward in the bifurcation diagram (*SI Appendix*, Fig. S4*C*). Thus, the region corresponding to cell-cycle arrest contracts in *SI Appendix*, Fig. S4*D*, whereas the region corresponding to apoptosis remains unchanged. Collectively, the determination of cell fate is controlled largely by p53 activity and is fine-tuned by multiple factors, thus allowing flexible control of cellular outcome.

Time Delay in Apoptosis Induction. Fig. 4 shows the temporal evolution of p53, p21, and Casp3 levels, with the initial concentrations being their steady-state levels at 10% serum without E1A. As *C* rises from 0.1 to 5.5%, the timing for full activation of proteins is increasingly delayed; for p53 and p21, it rises from hours to days with increasing *C*, because increasing the amount of growth factors enhances the expression of nuclear MDM2 and thus decreases the accumulation rate of p53 (17, 42). Casp3 activation depends on the slow accumulation of cytosolic Cyt *c*, which is promoted by Bax and Casp3, on rate-limiting steps such as apoptosome formation, and on antagonism between p21 and Casp3. Thus, the full activation of Casp3 is retarded more prominently, with the delay ranging from one to a few days. This delay has been well manifested experimentally (38).

Of note, cells first undergo cell-cycle arrest before commitment to apoptosis under low serum conditions; this sequence has physiological implications. This feature was observed previously in experiments with virus infection (38) or p53 overexpression (43). With E1A expression in serum-free systems, however, the initial p21-induced cell-cycle arrest at G2/M phase was not so remarkable (44). Possibly, the concentration of p21 preceding Casp3 activation does not reach a sufficiently high level, or p21 is rapidly cleaved by subsequently activated Casp3 before inducing a prominent arrest.

Two Stages in Apoptosis Induction upon Serum Starvation and Recovery. To unravel the influence of growth factors on apoptosis induction and the dynamics of Casp3 activation further, we devised a special case in which serum concentration is increased from a low to high level. We assume that the cell is first kept in a medium with 0.1% serum for a certain period (T) and then is supplied with 4% serum (Fig. 5*A*). Proapoptotic proteins accumulate during the starvation period, and there may exist a particular time beyond which Casp3 is always activated irrespective of serum. Indeed, if $T < T_0$ (~21.1 h), the activation of Casp3 is readily halted after serum recovery (Fig. 5*B*). As T approaches T_0, the activation process persists until its completion. For $T > T_0$, the activation process is more resistant to serum restoration. These results imply that apoptosis induction may involve the transition from a quenchable stage to an unquenchable stage.

Such a critical timing exists for other terminal serum concentrations; the T_0–C curve is roughly divided into three parts: left (0–2%), middle (2–5.5%), and right (5.5–10%). T_0 remains at 0 in the left region, indicating that cells always commit to

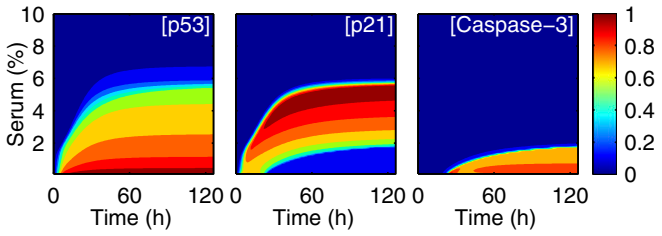

Fig. 4. Temporal evolution of protein levels. Time courses of the levels of p53, p21, and Casp3 in response to different serum stimuli (0–10%). Protein levels are normalized by their respective maxima.

apoptosis. T_0 rises slightly as C is increased from 2 to 5%. Surprisingly, T_0 is nearly a constant for $5.5 \le C \le 10\%$, markedly less than that in the middle region. This result seems to be incompatible with the bifurcation diagram in Fig. 3*A* showing Casp3 is inactivated for $C > 5.5\%$.

We found that another branch of stable fixed points exists for $5.5 \le C \le 10\%$ when the bifurcation diagram is plotted with different initial conditions (e.g., with a high Casp3 level) (Fig. 5*D*). This new branch still results from the positive feedback loops in the apoptosis module. Here, maintenance of high Casp3 levels does not require the sustained activation of p53/Bax, and activation of the caspase cascade is self-maintainable once being turned on (*SI Appendix*, Fig. S5). Notably, the threshold of Casp3 activation for $C \ge 5.5\%$ is markedly lower than that for $2 \le C < 5.5\%$ because p21 is expressed only at basal levels; thus, Casp3 activation can be initiated more easily.

Given that Casp3 levels depend largely on the amounts of free procasepse-3 and Cyt *c* in the cytosol, the dependence of T_0 on C can be interpreted as follows. If serum is restored to moderate concentrations, $p21_p$ will form a complex with procaspase-3 to inhibit Casp3 production. Only when Cyt *c* has accumulated sufficiently during a long starvation period can Casp3 activation persist, leading to cell apoptosis; otherwise, Casp3 decays to low levels, and cell-cycle arrest is induced (Fig. 5*E*). If serum is restored to high concentrations, p21 will be expressed at basal levels, and a large amount of procaspase-3 can be activated; thus, a relatively short starvation time is required for Cyt *c* elevation to induce apoptosis (otherwise, a very low amount of Cyt *c* leads to cell proliferation).

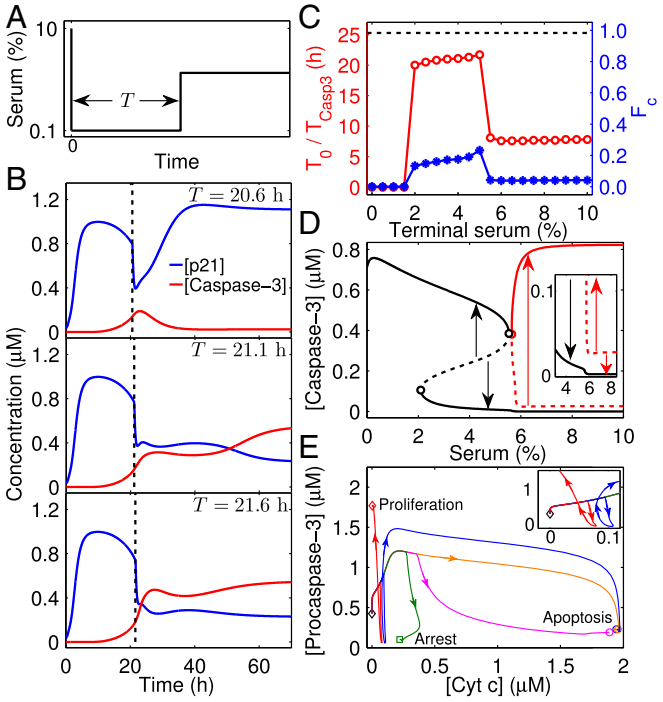

Fig. 5. Impact of serum recovery on apoptosis induction with fixed E1A expression. (*A*) Illustration of the simulation protocol. The cell is exposed to 0.1% serum for a period of T and is then to higher serum concentrations (e.g., 4%). (*B*) Critical T_0 for irreversible activation of Casp3. Time courses of [p21] and [Casp3] are shown for different starvation times: T = 20.6, 21.1, and 21.6 h. T_0 is ~21.1 h. (*C*) Dependence of T_0 (red circles) and F_C (blue stars) on terminal serum concentration. The dashed line denotes the required time (T_{Casp3}) for Casp3 activation when the cell is constantly exposed to 0.1% serum. (*D*) Full bifurcation diagram for Casp3 with the new branches denoted in red. An enlarged view is shown in the *Inset*. Arrows schematically denote the tendency of [Casp3] to progress to steady state when initiated from an unstable steady state. (*E*) Phase portraits of [Cyt *c*] and [procaspase-3] for different cases with C/T = 0.1%/+∞ (yellow), 3%/20.1 h (green), 3%/21.1 h (magenta), 8%/6.7 h (red), or 8%/8.7 h (blue). The *Inset* shows an enlarged view. The system begins with the steady state at 10% serum without E1A and ends at the steady state corresponding to proliferation, cell-cycle arrest, or apoptosis.

Two Waves of Cyt *c* Release. As shown above, sufficient accumulation of cytosolic Cyt *c* is essential for apoptosis induction. The release of Cyt *c* from mitochondria to the cytoplasm is assumed to follow biphasic dynamics (*SI Appendix*, *Method S3*, Eq. **S30**), so there exists a two-wave release during apoptosis, consistent with the experimental results (25, 26). The first wave engages a small pool of soluble Cyt *c* in the intermembrane space of mitochondria, whereas the second releases a large pool of Cyt *c*, which is evoked by the Casp3-mediated cleavage of mitochondrial complexes. The first wave is a slow process, whereas the second wave, Casp3-mediated amplification of Cyt *c* release, is a fast process associated with Casp3 activation (*SI Appendix*, Fig. S3).

The fraction of Cyt *c* released to the cytosol at $t = T_0$ (F_C) versus C parallels the T_0–C curve (Fig. 5*C*). F_C denotes the minimal fraction required for apoptosis induction. For $2 \le C \le 5\%$, F_C remains around 0.14, which is the fraction of soluble Cyt *c* that resides in mitochondria (45); the transition between two waves of Cyt *c* release roughly corresponds to the conversion between the two stages of apoptosis induction. In contrast, for $5.5 \le C \le 10\%$, F_C is less than 0.14, because a small amount of Cyt *c* is enough for apoptosis induction at a later time. Nevertheless, a long time is required for the full activation of Casp3 because free procaspase-3 is restored to high levels only after p21 is degraded to basal levels, and a sharp increase in Casp3 levels still corresponds to the initiation of the second wave of Cyt *c* release (see *SI Appendix*, Figs. S6 and S7 and analyses therein in terms of activation of the p21–Casp3 and Casp3–Cyt *c* release positive feedback loops). Of note, F_C would not be so small if more anti-apoptotic proteins such as Bcl-2 were included in the model.

The left boundary of the new branch in Fig. 5*D* is determined by the OFF-to-ON transition point of p53 in the bifurcation diagram (*SI Appendix*, Fig. S8*A*). When the kinetic mode of p53 converts from ultrasensitivity to bistability and the bistable regime enlarges, the region covered by this new branch expands leftward. Accordingly, the right parts of the T_0–C and F_C–C curves expand leftward (*SI Appendix*, Fig. S8*B*). Additionally, when each parameter is increased or decreased by 10% with respect to its default value, phenomena similar to those shown in Figs. 4 and 5 can be observed (*SI Appendix*, Fig. S9), suggesting that the main results described above are insensitive to parameter variations in a limited range.

Collectively, critical T_0 and F_C serve as a timer and a biomarker, respectively, for dictating the irreversibility of apoptosis induction; that is, E1A-expressing cells commit to apoptosis if the starvation time is longer than T_0 or if the fraction of released Cyt *c* exceeds F_C. The dependence of T_0 and F_C on terminal serum concentration reflects the extent to which apoptosis induction is resistant to serum readdition.

Discussion

The tumor-suppressive network enables appropriate cellular responses to mitogenic and oncogenic signals. We identify how key network components can dynamically contribute to tumor suppression. The discrimination between normal and oncogenic proliferative signaling is made via the all-or-none expression of ARF. Thus, cell-fate decisions can be reached by the competition of the proapoptotic and prosurvival signals through downstream functional modules, such as activated p53 in the cases of cell-cycle arrest and apoptosis.

Our results indicate that, in addition to p53, other regulators such as E2F1, p21, and Akt can affect cellular output. (*i*) Because

E2F1 has a critical proapoptotic role, E1A-expressing cells tend to suppress uncontrolled proliferation by inducing apoptosis. Alternatively ARF overexpression alone leads mostly to cell-cycle arrest (41). (*ii*) In the presence of p21/procaspase-3 interaction, cells may undergo apoptosis, cell-cycle arrest, or proliferation. Otherwise, cells could commit only apoptosis or proliferation. This inference is consistent with experimental observations (46). (*iii*) It is well-known that Akt promotes cell survival by engaging multiple pathways (6). For simplicity, we have limited our analysis to two loops, Akt–MDM2–p53–PTEN and p21–Casp3. They act either upstream or downstream of p53. Accordingly, Akt can modulate p53 levels via MDM2 and apoptosis induction via p21. Such a hierarchical organization of Akt signaling mediates its antiapoptotic function. Modulating the dynamics of and interactions between those proteins effectively controls the cellular outcome and may be exploited to find mechanisms to reactivate the tumor-suppressive functions in cancer cells.

Adding growth factors to serum-starved cells may evoke distinct cellular outcomes that will depend on the dynamics of serum recovery. Cells undergo cell-cycle arrest or apoptosis at moderate concentrations and proliferation or apoptosis at high concentrations. Apoptosis can be induced only when the starvation time is longer than a certain threshold, depending on the terminal serum concentration. These results depend on the antiapoptotic mechanism in the model: p21 can be phosphorylated by Akt to form a complex with procasepase-3, inhibiting its activation. Incorporating additional mechanisms, such as adding Bcl-2, may enrich our understanding of the impact of growth factors on apoptosis induction.

The proposed model provides insights into the role of the tumor-suppressive network in processing normal and oncogenic signals and making cell-fate decisions. Despite the multifaceted regulation of ARF at the transcriptional, translational, and posttranslational levels (47), the model focuses on the induction of ARF expression, because it is the main outcome of oncogenic signaling. The model could be extended to incorporate additional ARF regulation, so that we could gain more insights into delicate modulation of p53 and ARF activities.

ACKNOWLEDGMENTS. We thank Drs. Zhaohui Feng and Guang Yao for helpful discussions. This work was supported by 973 Program of China Grant 2013CB834104 and National Natural Science Foundation of China Grants 31361163003, 81421091, 11574139, and 11175084. J.N.O. was supported by National Science Foundation Grants PHY-1427654 and NSF-CHE 1614101 and by Cancer and Prevention Institute of Texas Grant R1110.

1. Hanahan D, Weinberg RA (2011) Hallmarks of cancer: The next generation. *Cell* 144: 646–674.
2. Lowe SW, Cepero E, Evan G (2004) Intrinsic tumour suppression. *Nature* 432:307–315.
3. Sherr CJ (2001) The INK4a/ARF network in tumour suppression. *Nat Rev Mol Cell Biol* 2:731–737.
4. Sherr CJ (1998) Tumor surveillance via the ARF-p53 pathway. *Genes Dev* 12: 2984–2991.
5. Levine AJ, Oren M (2009) The first 30 years of p53: Growing ever more complex. *Nat Rev Cancer* 9:749–758.
6. Datta SR, Brunet A, Greenberg ME (1999) Cellular survival: A play in three Akts. *Genes Dev* 13:2905–2927.
7. Polager S, Ginsberg D (2009) p53 and E2f: Partners in life and death. *Nat Rev Cancer* 9:738–748.
8. Lowe SW, Ruley HE (1993) Stabilization of the p53 tumor suppressor is induced by adenovirus 5 E1A and accompanies apoptosis. *Genes Dev* 7:535–545.
9. Harrington EA, Bennett MR, Fanidi A, Evan GI (1994) c-Myc-induced apoptosis in fibroblasts is inhibited by specific cytokines. *EMBO J* 13:3286–3295.
10. Canman CE, Gilmer TM, Coutts SB, Kastan MB (1995) Growth factor modulation of p53-mediated growth arrest versus apoptosis. *Genes Dev* 9:600–611.
11. Deng J, Xia W, Hung MC (1998) Adenovirus 5 E1A-mediated tumor suppression associated with E1A-mediated apoptosis *in vivo*. *Oncogene* 17:2167–2175.
12. Yao G, Lee TJ, Mori S, Nevins JR, You L (2008) A bistable Rb-E2F switch underlies the restriction point. *Nat Cell Biol* 10:476–482.
13. de Stanchina E, et al. (1998) E1A signaling to p53 involves the $p19^{ARF}$ tumor suppressor. *Genes Dev* 12:2434–2442.
14. Komori H, Enomoto M, Nakamura M, Iwanaga R, Ohtani K (2005) Distinct E2F-mediated transcriptional program regulates $p14^{ARF}$ gene expression. *EMBO J* 24: 3724–3736.
15. Stott FJ, et al. (1998) The alternative product from the human *CDKN2A* locus, $p14^{ARF}$, participates in a regulatory feedback loop with p53 and MDM2. *EMBO J* 17: 5001–5014.
16. Ries S, et al. (2000) Opposing effects of Ras on p53: Transcriptional activation of *mdm2* and induction of $p19^{ARF}$. *Cell* 103:321–330.
17. Zhou BP, et al. (2001) *HER-2/neu* induces p53 ubiquitination via Akt-mediated MDM2 phosphorylation. *Nat Cell Biol* 3:973–982.
18. Mayo LD, Donner DB (2001) A phosphatidylinositol 3-kinase/Akt pathway promotes translocation of Mdm2 from the cytoplasm to the nucleus. *Proc Natl Acad Sci USA* 98: 11598–11603.
19. Stambolic V, et al. (2001) Regulation of PTEN transcription by p53. *Mol Cell* 8:317–325.
20. Stambolic V, et al. (1998) Negative regulation of PKB/Akt-dependent cell survival by the tumor suppressor PTEN. *Cell* 95:29–39.
21. Wee KB, Aguda BD (2006) Akt versus p53 in a network of oncogenes and tumor suppressor genes regulating cell survival and death. *Biophys J* 91:857–865.
22. Miyashita T, Reed JC (1995) Tumor suppressor p53 is a direct transcriptional activator of the human bax gene. *Cell* 80:293–299.
23. Nahle Z, et al. (2002) Direct coupling of the cell cycle and cell death machinery by E2F. *Nat Cell Biol* 4:859–864.
24. Kirsch DG, et al. (1999) Caspase-3-dependent cleavage of Bcl-2 promotes release of cytochrome c. *J Biol Chem* 274:21155–21161.
25. Garrido C, et al. (2006) Mechanisms of cytochrome c release from mitochondria. *Cell Death Differ* 13:1423–1433.
26. Chen Q, Gong B, Almasan A (2000) Distinct stages of cytochrome c release from mitochondria: Evidence for a feedback amplification loop linking caspase activation to mitochondrial dysfunction in genotoxic stress induced apoptosis. *Cell Death Differ* 7:227–233.
27. Zhou BP, et al. (2001) Cytoplasmic localization of $p21^{Cip1/WAF1}$ by Akt-induced phosphorylation in HER-2/neu-overexpressing cells. *Nat Cell Biol* 3:245–252.
28. Child ES, Mann DJ (2006) The intricacies of p21 phosphorylation: Protein/protein interactions, subcellular localization and stability. *Cell Cycle* 5:1313–1319.
29. Zhang Y, Fujita N, Tsuruo T (1999) Caspase-mediated cleavage of $p21^{Waf1/Cip1}$ converts cancer cells from growth arrest to undergoing apoptosis. *Oncogene* 18:1131–1138.
30. Zhang XP, Liu F, Wang W (2011) Two-phase dynamics of p53 in the DNA damage response. *Proc Natl Acad Sci USA* 108:8990–8995.
31. Li C, Wang J (2014) Quantifying the underlying landscape and paths of cancer. *J R Soc Interface* 11:20140774.
32. Yu C, Wang J (2016) A physical mechanism and global quantification of breast cancer. *PLoS One* 11:e0157422.
33. Li C, Wang J (2015) Quantifying the landscape for development and cancer from a core cancer stem cell circuit. *Cancer Res* 75:2607–2618.
34. Lowe SW, Sherr CJ (2003) Tumor suppression by Ink4a-Arf: Progress and puzzles. *Curr Opin Genet Dev* 13:77–83.
35. Iaquinta PJ, Aslanian A, Lees JA (2005) Regulation of the *Arf/p53* tumor surveillance network by E2F. *Cold Spring Harb Symp Quant Biol* 70:309–316.
36. Ogawara Y, et al. (2002) Akt enhances Mdm2-mediated ubiquitination and degradation of p53. *J Biol Chem* 277:21843–21850.
37. Debbas M, White E (1993) Wild-type p53 mediates apoptosis by E1A, which is inhibited by E1B. *Genes Dev* 7:546–554.
38. Sabbatini P, McCormick F (1999) Phosphoinositide 3-OH kinase (PI3K) and PKB/Akt delay the onset of p53-mediated, transcriptionally dependent apoptosis. *J Biol Chem* 274:24263–24269.
39. Hershko T, Chaussepied M, Oren M, Ginsberg D (2005) Novel link between E2F and p53: Proapoptotic cofactors of p53 are transcriptionally upregulated by E2F. *Cell Death Differ* 12:377–383.
40. Rao L, et al. (1992) The adenovirus E1A proteins induce apoptosis, which is inhibited by the E1B 19-kDa and Bcl-2 proteins. *Proc Natl Acad Sci USA* 89:7742–7746.
41. Quelle DE, Zindy F, Ashmun RA, Sherr CJ (1995) Alternative reading frames of the *INK4a* tumor suppressor gene encode two unrelated proteins capable of inducing cell cycle arrest. *Cell* 83:993–1000.
42. Ashcroft M, et al. (2002) Phosphorylation of HDM2 by Akt. *Oncogene* 21:1955–1962.
43. Kracikova M, Akiri G, George A, Sachidanandam R, Aaronson SA (2013) A threshold mechanism mediates p53 cell fate decision between growth arrest and apoptosis. *Cell Death Differ* 20:576–588.
44. Sabbatini P, Lin J, Levine AJ, White E (1995) Essential role for p53-mediated transcription in E1A-induced apoptosis. *Genes Dev* 9:2184–2192.
45. Scorrano L, et al. (2002) A distinct pathway remodels mitochondrial cristae and mobilizes cytochrome c during apoptosis. *Dev Cell* 2:55–67.
46. Gorospe M, et al. (1997) $p21^{Waf1/Cip1}$ protects against p53-mediated apoptosis of human melanoma cells. *Oncogene* 14:929–935.
47. Gil J, Peters G (2006) Regulation of the *INK4b-ARF-INK4a* tumour suppressor locus: All for one or one for all. *Nat Rev Mol Cell Biol* 7:667–677.

SI Appendix

Modeling the response of a tumor-suppressive network to mitogenic and oncogenic signals

I. SI Appendix Methods

Method S1: Details of the model

The model comprises three modules. In the following, we describe each module in detail.

1. Regulation of cell proliferation (Fig. S1*B*)

The central node of this module is activator E2F (E2F1, E2F2 and E2F3A), transactivating genes involved in cell cycle entry and DNA replication. The E2F-RB pathway is responsible for the control of the restriction (*R*) point. In quiescent cells, RB remains in a hypo-phosphorylated status and actively represses the transcriptional activity of E2F by blocking its transactivation domain (TD). Upon serum stimulation, cyclin D is induced by growth factors or Myc and forms a complex with Cdk4/6 to phosphorylate RB, which releases E2F from the repression by RB. Myc also induces the production of E2F. E2F facilitates its own activation through two positive feedback loops: E2F transactivates cyclin E, and cyclin E/Cdk2 phosphorylates RB, which further releases E2F; E2F also mediates its own transcription. Because of these positive feedback loops, E2F exhibits bistability in response to serum stimulation[1].

The framework of this module is derived from Ref. 1, and recent experimental advances are incorporated to differentiate E2F1 from other activator E2Fs (E2F2 and E2F3A). There are three major revisions: 1) The active E2F1 released from RB's inhibition by E1A remains in the E1A-RB complex through the interaction between E2F1 and RB[2,3]; 2) the cyclin-mediated phosphorylation of RB only releases the TD of E2F1 from RB, but E2F1 still associates with RB through the interaction between its Marked Box and a C-terminal region of RB[4]; 3) both E1A and RB protect activator E2F from degradation[5,6] and associate with E2F to form the E1A-E2F and RB-E2F complexes[7,8]. Additionally, E1A stabilizes RB through their interactions[2]. Phosphorylated RB is resistant to binding E1A[9].

2. p53 activation (Fig. S1*C*)

There are two opposing factors regulating p53 expression through MDM2—ARF and Akt. Growth factors (GFs) in serum promote the transcription of *mdm2*[10] and Akt activation via phosphorylation. Active Akt phosphorylates MDM2, enhancing its nuclear accumulation. As a transcriptional target of p53, MDM2 in turn targets p53 for degradation. p53 induces the production of PTEN[11], a phosphatase that dephosphorylates the PIP3 kinase, which is required for the activation of Akt[12]. Thus, Akt, MDM2, p53 and PTEN enclose a positive feedback loop. On the other hand, ARF blocks the E3 ligase activity of MDM2 toward p53. Notably, the interaction between MDM2 and ARF is

significantly stronger than that between $MDM2_p$ and ARF[13].

3. Apoptosis induction by p53 and E2F1 (Fig. S1*D*)

We focus on the intrinsic apoptotic pathway, which triggers apoptosis in a mitochondria-dependent manner. The caspase-activation cascade makes up the backbone of the module. The active Bax protein is able to form pores in the outer membrane of mitochondria, leading to the release of cytochrome *c* (Cyt *c*) from mitochondria to the cytoplasm[14-17]. Released Cyt *c* then binds to and activates Apaf-1 (apoptotic protease-activating factor-1) to form the caspase-activating complex, apoptosome[18,19]. Recruited to the apoptosome, procaspase-9 forms dimers, undergoes autoprocessing and becomes proteolytically active. The active caspase-9 dimer, either free or bound to the apoptosome, then leads to activation of the executor caspase-3[19,22,23]. Furthermore, active caspase-3 promotes the release of Cyt *c*. Specifically, the ratio of caspase-9 to apoptosome is 1:1, and the activated caspase-9 dimer on apoptosome can continuously be displaced by procaspase-9[20,21].

E2F1 promotes apoptosis through inducing the production of Apaf-1, procaspase-9 and procaspase-3[22], while p53 induces Bax and thus initiates the apoptotic program[23]. p21, induced by p53, is able to interact with procaspase-3 to block its activation. Active caspase-3 in turn catalyzes the cleavage and inactivation of p21. Some redundant regulatory pathways, especially anti-apoptotic proteins and their interactions (e.g., p53/Bcl-2/Bax and Smac/IAPs/caspase pathways), are omitted here.

The bistability and threshold-crossing mechanisms underlying the action of effector caspases have been explored extensively[24-26]. In our model, this feature is imparted by two positive feedback loops. One is the caspase-3-mediated amplification of Cyt *c* release, and the other involves the interactions between p21, $p21_p$, procaspase-3 and caspase-3. The caspase-3-mediated mitochondrial amplification loop is engaged in ARF-dependent apoptosis[27].

Method S2: Interpretations of the functions of proteins

1. Function and regulation of the ARF tumor suppressor

The ARF protein is a major factor linking the RB-E2F and MDM2-p53 pathways. ARF is encoded in part by an alternative reading frame within the second of three exons that comprise the *INK4A* gene. Particularly, the *Arf* gene is not expressed in most normal tissues, but induced upon oncogenic signals. ARF activates the p53-mediated tumor suppressive program through antagonizing the E3 ligase activity of MDM2[28].

In human cells, the transcriptional activation of ARF is mainly attributed to activator E2F[29]. In unstressed cells, the *Arf* promoter is actively suppressed by E2F3B or Bim-1[30-32], which buffers against the transcriptional activity of activator E2F. As cells are infected with E1A, this adenovirus protein functions through multiple ways to induce cell transformation, and a dominant one is to disrupt the elegantly controlled RB-E2F interaction[33-35], which results in ectopic expression of E2F[2]. The binding of hyper-activated E2F to the *Arf* promoter overrides that of repressors, leading to induction of ARF.

2. Cell-cycle arrest triggered by p53

It is well known that the p53 protein can induce G1 cell-cycle arrest in response to multiple cellular stresses, and this role is primarily related to p21[36,37]. p21 binds and inactivates cyclin E/Cdk2, resulting in RB hypo-phosphorylation and activation[38]. Then, activated RB induces the G1 arrest by negative regulation of activator E2F[39], which mediates the transcription of multiple genes that are crucial for S phase entry and cell cycle progression[40]. Here, RB is inhibited or blocked by E1A irrespective of its phosphorylation status; thus, the G1/S checkpoint is disrupted, with the ectopic expression of E2F and a lack of G1/S arrest.

In addition to G1 arrest, p53 also contributes to G2/M arrest by inducing the transcription of genes like p21 and 14-3-3. Such cell cycle arresters converge to inhibit the activation of Cdc2, which is responsible for G2/M phase transition[41-44].

3. Pro-apoptotic roles of p53 and E2F1

Upon full activation, both p53 and E2F1 have a pro-apoptotic role. Accumulating evidence suggests that they cooperate to induce apoptosis[45,46]. In addition to E2F1-induced activation of p53 through the E2F-ARF-MDM2 axis, p53 and E2F1 regulate a plethora of target genes. First, they separately transactivate some major pro-apoptotic genes, and these gene products promote apoptosis cooperatively. For example, E2F1 transactivates the expression of procaspase-9 and procaspase-3[22],

while p53 upregulates the expression of Bax[23]. Second, genes like Aparf-1 and PUMA are transcriptionally activated by both E2F1 and p53[47-49], while several anti-apoptotic genes, like some Bcl-2 family members, are negatively regulated by both E2F1 and p53[50-53].

4. Anti-apoptotic and pro-survival roles of Akt

Akt is well known for its pro-survival role and hyperactivity across various tumors. It is activated by the PI3K pathway and mediates the pro-survival signals emanating from diverse extracellular growth or survival signals, such as insulin and growth factors[54,55]. Once activated, Akt functions through multiple and somewhat redundant pathways (Fig. S1*A*). The pathways included in our model are described in the following:

a. Phosphorylation of p21. The phosphorylation at T145 by Akt is one of the best characterized posttranslational modifications of p21. The phosphorylation induces the relocalization of p21 from the nucleus to the cytoplasm[56,57], where it is exposed to a wide range of binding partners, one of which is procaspase-3. The interaction between p21 and procaspase-3 blocks the proteolytic activation of procaspase-3[58,59]. Here, it is assumed that phosphorylated p21 is evenly distributed between the nucleus and cytoplasm; thus, it functions as a cell-cycle arrester through inhibiting Cdks and an apoptotic inhibitor through repressing procaspase-3 activation. In contrast, dephosphorylated p21 resides exclusively in the nucleus, functioning as a cell-cycle arrester.

b. Phosphorylation of MDM2. The phosphorylation of MDM2 by Akt leads to its nuclear accumulation, strengthening its inhibition of p53[13,60,61]. Here, it is assumed that dephosphorylated MDM2 is evenly distributed between the cytoplasm and nucleus, with the same nuclear import and export activity, and phosphorylated MDM2 is mainly located in the nucleus, with the ability to interact with ARF significantly weakened[13,61].

5. The p21/caspase-3 interaction

Phosphorylated p21 can accumulate in the cytoplasm[56,57], where it interacts with diverse binding partners, such as procaspase-3 (Pro3). p21 binds to Pro3 through its N-terminal and prevents the conversion of Pro3 to mature caspase-3 (Casp3), thus dampening apoptosis[58,59]. This anti-apoptotic role of p21 is involved in apoptosis induced by p53[62,63] and by ARF[27,64,65]. Activated Casp3 mediates the cleavage and inactivation of p21[66,67], which is an early event in p53-dependent apoptosis. Thus, the p21/Casp3 interaction forms a positive feedback loop which sensitizes cells to both pro-survival and -apoptotic signals.

6. Biphasic release of cytochrome *c*

Accumulating data suggest that Cyt *c* release follows biphasic kinetics[68,69]. The first wave of Cyt *c* release, preceding caspase activation, involves a small pool of soluble Cyt *c* in the intermembrane space (~14% of mitochondrial Cyt *c*). The second wave releases a large pool of Cyt *c* that is normally sequestered by cardiolipin (CL) on the inner membrane and is released upon CL oxidation, which is provoked by the Casp3-mediated cleavage of mitochondrial complexes and increase in ROS, e.g. the Casp3-mediated cleavage of p75 subunit of the respiratory complex I or cytochrome c1[70,71].

Method S3: ODEs of the model

Module 1: Regulation of cell proliferation

Case *A*: Normal growth condition—cell cycle is stimulated by growth factors (GFs)

$$\frac{d[\mathrm{Myc}]}{dt}=\frac{k_{\mathrm{M\_S}}[S]}{K_{\mathrm{S}}+[S]}+k_{\mathrm{M\_E}}\left(\frac{[\mathrm{E2F1}]+[\mathrm{E2Fs}]}{K_{\mathrm{E}}+[\mathrm{E2F1}]+[\mathrm{E2Fs}]}\right)+k_{\mathrm{M\_E}}\left(\frac{[\mathrm{R_pE}]}{K_{\mathrm{RpE}}+[\mathrm{R_pE}]}\right)-d_{\mathrm{Myc}}[\mathrm{Myc}] \tag{S1a}$$

$$\frac{d[\mathrm{CycD}]}{dt}=\frac{k_{\mathrm{CD\_S}}[S]}{K_{\mathrm{S}}+[S]}+\frac{k_{\mathrm{CD\_M}}[\mathrm{Myc}]}{K_{\mathrm{M}}+[\mathrm{Myc}]}-d_{\mathrm{CD}}[\mathrm{CycD}] \tag{S2a}$$

$$\frac{d[\mathrm{CycE}]}{dt}=k_{\mathrm{CE\_E}}\left(\frac{[\mathrm{E2F1}]+[\mathrm{E2Fs}]}{K_{\mathrm{E}}+[\mathrm{E2F1}]+[\mathrm{E2Fs}]}\right)+k_{\mathrm{CE\_E}}\left(\frac{[\mathrm{R_pE}]}{K_{\mathrm{RpE}}+[\mathrm{R_pE}]}\right)-d_{\mathrm{CE}}[\mathrm{CycE}] \tag{S3a}$$

$$\begin{aligned}\frac{d[\mathrm{E2F1}]}{dt}=&k_{\mathrm{E2F}}+\frac{k_{\mathrm{E\_M}}[\mathrm{Myc}]}{K_{\mathrm{M}}+[\mathrm{Myc}]}+k_{\mathrm{E\_E}}\left(\frac{[\mathrm{Myc}]}{K_{\mathrm{M}}+[\mathrm{Myc}]}\right)\left(\frac{[\mathrm{E2F1}]+[\mathrm{E2Fs}]}{K_{\mathrm{E}}+[\mathrm{E2F1}]+[\mathrm{E2Fs}]}\right)+\\&k_{\mathrm{E\_E}}\left(\frac{[\mathrm{Myc}]}{K_{\mathrm{M}}+[\mathrm{Myc}]}\right)\left(\frac{[\mathrm{R_pE}]}{K_{\mathrm{RpE}}+[\mathrm{R_pE}]}\right)+D_{\mathrm{RpE}}[\mathrm{R_pE}]-k_{\mathrm{RE}}[\mathrm{RB}][\mathrm{E2F1}]-k_{\mathrm{RpE}}[\mathrm{RB_p}][\mathrm{E2F1}]-d_{\mathrm{E2F}}[\mathrm{E2F1}]\end{aligned} \tag{S4a}$$

$$\begin{aligned}\frac{d[\mathrm{E2Fs}]}{dt}=&k_{\mathrm{E2F}}+\frac{k_{\mathrm{E\_M}}[\mathrm{Myc}]}{K_{\mathrm{M}}+[\mathrm{Myc}]}+k_{\mathrm{E\_E}}\left(\frac{[\mathrm{Myc}]}{K_{\mathrm{M}}+[\mathrm{Myc}]}\right)\left(\frac{[\mathrm{E2F1}]+[\mathrm{E2Fs}]}{K_{\mathrm{E}}+[\mathrm{E2F1}]+[\mathrm{E2Fs}]}\right)\\&+k_{\mathrm{E\_E}}\left(\frac{[\mathrm{Myc}]}{K_{\mathrm{M}}+[\mathrm{Myc}]}\right)\left(\frac{[\mathrm{R_pE}]}{K_{\mathrm{RpE}}+[\mathrm{R_pE}]}\right)+\frac{k_{\mathrm{p\_RE}}[\mathrm{CycD}][\mathrm{REs}]}{K_{\mathrm{CD}}+[\mathrm{REs}]}+\frac{k_{\mathrm{p\_RE}}[\mathrm{CycE}][\mathrm{REs}]}{K_{\mathrm{CE}}+[\mathrm{REs}]}\\&-k_{\mathrm{RE}}[\mathrm{RB}][\mathrm{E2Fs}]-d_{\mathrm{E2F}}[\mathrm{E2Fs}]\end{aligned} \tag{S5a}$$

$$\frac{d[\mathrm{RE}]}{dt}=k_{\mathrm{RE}}[\mathrm{RB}][\mathrm{E2F1}]+\frac{k_{\mathrm{DP2}}[\mathrm{R_pE}]}{K_{\mathrm{RpE}}+[\mathrm{R_pE}]}-\frac{k_{\mathrm{p\_RE}}[\mathrm{CycD}][\mathrm{RE}]}{K_{\mathrm{CD}}+[\mathrm{RE}]}-\frac{k_{\mathrm{p\_RE}}[\mathrm{CycE}][\mathrm{RE}]}{K_{\mathrm{CE}}+[\mathrm{RE}]}-d_{\mathrm{RE}}[\mathrm{RE}] \tag{S6a}$$

$$\frac{d[\mathrm{REs}]}{dt}=k_{\mathrm{RE}}[\mathrm{RB}][\mathrm{E2Fs}]-\frac{k_{\mathrm{p\_RE}}[\mathrm{CycD}][\mathrm{REs}]}{K_{\mathrm{CD}}+[\mathrm{REs}]}-\frac{k_{\mathrm{p\_RE}}[\mathrm{CycE}][\mathrm{REs}]}{K_{\mathrm{CE}}+[\mathrm{REs}]}-d_{\mathrm{RE}}[\mathrm{REs}] \tag{S7a}$$

$$\frac{d[\mathrm{R_pE}]}{dt}=\frac{k_{\mathrm{p\_RE}}[\mathrm{CycD}][\mathrm{RE}]}{K_{\mathrm{CD}}+[\mathrm{RE}]}+\frac{k_{\mathrm{p\_RE}}[\mathrm{CycE}][\mathrm{RE}]}{K_{\mathrm{CE}}+[\mathrm{RE}]}+k_{\mathrm{RpE}}[\mathrm{RB_p}][\mathrm{E2F1}]-\frac{k_{\mathrm{DP2}}[\mathrm{R_pE}]}{K_{\mathrm{RpE}}+[\mathrm{R_pE}]}-D_{\mathrm{RpE}}[\mathrm{R_pE}]-d_{\mathrm{RpE}}[\mathrm{R_pE}] \tag{S8a}$$

$$\frac{d[\mathrm{RB}]}{dt}=k_{\mathrm{RB}}+\frac{k_{\mathrm{DP1}}[\mathrm{RB_p}]}{K_{\mathrm{RBp}}+[\mathrm{RB_p}]}-\frac{k_{\mathrm{p\_RB}}[\mathrm{CycD}][\mathrm{RB}]}{K_{\mathrm{CD}}+[\mathrm{RB}]}-\frac{k_{\mathrm{p\_RB}}[\mathrm{CycE}][\mathrm{RB}]}{K_{\mathrm{CE}}+[\mathrm{RB}]}-k_{\mathrm{RE}}[\mathrm{RB}]\left([\mathrm{E2F1}]+[\mathrm{E2Fs}]\right)-d_{\mathrm{RB}}[\mathrm{RB}] \tag{S9a}$$

$$\frac{d[\mathrm{RB_p}]}{dt}=\frac{k_{\mathrm{p\_RB}}[\mathrm{CycD}][\mathrm{RB}]}{K_{\mathrm{CD}}+[\mathrm{RB}]}+\frac{k_{\mathrm{p\_RB}}[\mathrm{CycE}][\mathrm{RB}]}{K_{\mathrm{CE}}+[\mathrm{RB}]}+\frac{k_{\mathrm{p\_RE}}[\mathrm{CycD}][\mathrm{REs}]}{K_{\mathrm{CD}}+[\mathrm{REs}]}+\frac{k_{\mathrm{p\_RE}}[\mathrm{CycE}][\mathrm{REs}]}{K_{\mathrm{CE}}+[\mathrm{REs}]}+ D_{\mathrm{RpE}}[\mathrm{R_pE}]-\frac{k_{\mathrm{DP1}}[\mathrm{RB_p}]}{K_{\mathrm{RBp}}+[\mathrm{RB_p}]}-k_{\mathrm{RpE}}[\mathrm{RB_p}][\mathrm{E2F1}]-d_{\mathrm{RBp}}[\mathrm{RB_p}] \tag{S10a}$$

$$\frac{d[\mathrm{ARF}]}{dt}=k_{\mathrm{A\_E}}\left(\frac{([\mathrm{E2F1}]+[\mathrm{E2Fs}])^3}{K_{\mathrm{A\_E}}^3+([\mathrm{E2F1}]+[\mathrm{E2Fs}])^3}\right)+k_{\mathrm{A\_RpE}}\left(\frac{[\mathrm{R_pE}]^3}{K_{\mathrm{A\_RpE}}^3+[\mathrm{R_pE}]^3}\right)+ D_{\mathrm{MpA}}[\mathrm{M_pA}]+D_{\mathrm{MA}}[\mathrm{MA}]-k_{\mathrm{MpA}}[\mathrm{MDM2_p}][\mathrm{ARF}]-k_{\mathrm{MA}}[\mathrm{MDM2}][\mathrm{ARF}]-d_{\mathrm{ARF}}[\mathrm{ARF}] \tag{S11a}$$

Case *B*: Oncogenic condition—cell cycle is stimulated by GFs and/or E1A

$$\frac{d[\mathrm{Myc}]}{dt}=\frac{k_{\mathrm{M\_S}}[S]}{K_{\mathrm{S}}+[S]}+k_{\mathrm{M\_E}}\left(\frac{[\mathrm{E2F1}]+[\mathrm{E2Fs}]}{K_{\mathrm{E}}+[\mathrm{E2F1}]+[\mathrm{E2Fs}]}\right)+k_{\mathrm{M\_E}}\left(\frac{[\mathrm{E1E1}]+[\mathrm{EsE1}]}{K_{\mathrm{EE1}}+[\mathrm{E1E1}]+[\mathrm{EsE1}]}\right)+ k_{\mathrm{M\_E}}\left(\frac{[\mathrm{REE1}]}{K_{\mathrm{REE1}}+[\mathrm{REE1}]}\right)+k_{\mathrm{M\_E}}\left(\frac{[\mathrm{R_pE}]}{K_{\mathrm{RpE}}+[\mathrm{R_pE}]}\right)-d_{\mathrm{Myc}}[\mathrm{Myc}] \tag{S1b}$$

$$\frac{d[\mathrm{CycD}]}{dt}=\frac{k_{\mathrm{CD\_S}}[S]}{K_{\mathrm{S}}+[S]}+\frac{k_{\mathrm{CD\_M}}[\mathrm{Myc}]}{K_{\mathrm{M}}+[\mathrm{Myc}]}-d_{\mathrm{CD}}[\mathrm{CycD}] \tag{S2b}$$

$$\frac{d[\mathrm{CycE}]}{dt}=k_{\mathrm{CE\_E}}\left(\frac{[\mathrm{E2F1}]+[\mathrm{E2Fs}]}{K_{\mathrm{E}}+[\mathrm{E2F1}]+[\mathrm{E2Fs}]}\right)+k_{\mathrm{CE\_E}}\left(\frac{[\mathrm{E1E1}]+[\mathrm{EsE1}]}{K_{\mathrm{EE1}}+[\mathrm{E1E1}]+[\mathrm{EsE1}]}\right)+ k_{\mathrm{CE\_E}}\left(\frac{[\mathrm{R_pE}]}{K_{\mathrm{RpE}}+[\mathrm{R_pE}]}\right)+k_{\mathrm{CE\_E}}\left(\frac{[\mathrm{REE1}]}{K_{\mathrm{REE1}}+[\mathrm{REE1}]}\right)-d_{\mathrm{CE}}[\mathrm{CycE}] \tag{S3b}$$

$$\frac{d[\mathrm{E2F1}]}{dt}=k_{\mathrm{E2F}}+\frac{k_{\mathrm{E\_M}}[\mathrm{Myc}]}{K_{\mathrm{M}}+[\mathrm{Myc}]}+k_{\mathrm{E\_E}}\left(\frac{[\mathrm{Myc}]}{K_{\mathrm{M}}+[\mathrm{Myc}]}\right)\left(\frac{[\mathrm{E2F1}]+[\mathrm{E2Fs}]}{K_{\mathrm{E}}+[\mathrm{E2F1}]+[\mathrm{E2Fs}]}\right)+ k_{\mathrm{E\_E}}\left(\frac{[\mathrm{Myc}]}{K_{\mathrm{M}}+[\mathrm{Myc}]}\right)\left(\frac{[\mathrm{E1E1}]+[\mathrm{EsE1}]}{K_{\mathrm{EE1}}+[\mathrm{E1E1}]+[\mathrm{EsE1}]}\right)+ k_{\mathrm{E\_E}}\left(\frac{[\mathrm{Myc}]}{K_{\mathrm{M}}+[\mathrm{Myc}]}\right)\left(\frac{[\mathrm{R_pE}]}{K_{\mathrm{RpE}}+[\mathrm{R_pE}]}\right)+k_{\mathrm{E\_E}}\left(\frac{[\mathrm{Myc}]}{K_{\mathrm{M}}+[\mathrm{Myc}]}\right)\left(\frac{[\mathrm{REE1}]}{K_{\mathrm{REE1}}+[\mathrm{REE1}]}\right)+ D_{\mathrm{RpE}}[\mathrm{R_pE}]+D_{\mathrm{REE1}}[\mathrm{REE1}]+D_{\mathrm{EE1}}[\mathrm{E1E1}]-k_{\mathrm{RE}}[\mathrm{RB}][\mathrm{E2F1}]-k_{\mathrm{RpE}}[\mathrm{RB_p}][\mathrm{E2F1}]- k_{\mathrm{EE1}}[\mathrm{E2F1}][\mathrm{E1A}]-k_{\mathrm{REE1}}[\mathrm{RE1}][\mathrm{E2F1}]-d_{\mathrm{E2F}}[\mathrm{E2F1}] \tag{S4b}$$

$$\frac{d[\mathrm{E2Fs}]}{dt}=k_{\mathrm{E2F}}+\frac{k_{\mathrm{E\_M}}[\mathrm{Myc}]}{K_{\mathrm{M}}+[\mathrm{Myc}]}+k_{\mathrm{E\_E}}\left(\frac{[\mathrm{Myc}]}{K_{\mathrm{M}}+[\mathrm{Myc}]}\right)\left(\frac{[\mathrm{E2F1}]+[\mathrm{E2Fs}]}{K_{\mathrm{E}}+[\mathrm{E2F1}]+[\mathrm{E2Fs}]}\right)+ k_{\mathrm{E\_E}}\left(\frac{[\mathrm{Myc}]}{K_{\mathrm{M}}+[\mathrm{Myc}]}\right)\left(\frac{[\mathrm{E1E1}]+[\mathrm{EsE1}]}{K_{\mathrm{EE1}}+[\mathrm{E1E1}]+[\mathrm{EsE1}]}\right)+k_{\mathrm{E\_E}}\left(\frac{[\mathrm{Myc}]}{K_{\mathrm{M}}+[\mathrm{Myc}]}\right)\left(\frac{[\mathrm{R_pE}]}{K_{\mathrm{RpE}}+[\mathrm{R_pE}]}\right)+ k_{\mathrm{E\_E}}\left(\frac{[\mathrm{Myc}]}{K_{\mathrm{M}}+[\mathrm{Myc}]}\right)\left(\frac{[\mathrm{REE1}]}{K_{\mathrm{REE1}}+[\mathrm{REE1}]}\right)+\frac{k_{\mathrm{p\_RE}}[\mathrm{CycD}][\mathrm{REs}]}{K_{\mathrm{CD}}+[\mathrm{REs}]}+\frac{k_{\mathrm{p\_RE}}[\mathrm{CycE}][\mathrm{REs}]}{K_{\mathrm{CE}}+[\mathrm{REs}]}+ k_{\mathrm{RE1}}[\mathrm{REs}][\mathrm{E1A}]+D_{\mathrm{EE1}}[\mathrm{EsE1}]-k_{\mathrm{RE}}[\mathrm{RB}][\mathrm{E2Fs}]-k_{\mathrm{EE1}}[\mathrm{E2Fs}][\mathrm{E1A}]-d_{\mathrm{E2F}}[\mathrm{E2Fs}] \tag{S5b}$$

$$\frac{d[\mathrm{RE}]}{dt} = k_{\mathrm{RE}}[\mathrm{RB}][\mathrm{E2F1}] + \frac{k_{\mathrm{DP2}}[\mathrm{R_pE}]}{K_{\mathrm{DRpE}}+[\mathrm{R_pE}]} - \frac{k_{\mathrm{p\_RE}}[\mathrm{CycD}][\mathrm{RE}]}{K_{\mathrm{CD}}+[\mathrm{RE}]} - \frac{k_{\mathrm{p\_RE}}[\mathrm{CycE}][\mathrm{RE}]}{K_{\mathrm{CE}}+[\mathrm{RE}]} - k_{\mathrm{RE1}}[\mathrm{RE}][\mathrm{E1A}] - d_{\mathrm{RE}}[\mathrm{RE}] \quad \text{(S6b)}$$

$$\frac{d[\mathrm{REs}]}{dt} = k_{\mathrm{RE}}[\mathrm{RB}][\mathrm{E2Fs}] - \frac{k_{\mathrm{p\_RE}}[\mathrm{CycD}][\mathrm{REs}]}{K_{\mathrm{CD}}+[\mathrm{REs}]} - \frac{k_{\mathrm{p\_RE}}[\mathrm{CycE}][\mathrm{REs}]}{K_{\mathrm{CE}}+[\mathrm{REs}]} - k_{\mathrm{RE1}}[\mathrm{REs}][\mathrm{E1A}] - d_{\mathrm{RE}}[\mathrm{REs}] \quad \text{(S7b)}$$

$$\frac{d[\mathrm{R_pE}]}{dt} = \frac{k_{\mathrm{p\_RE}}[\mathrm{CycD}][\mathrm{RE}]}{K_{\mathrm{CD}}+[\mathrm{RE}]} + \frac{k_{\mathrm{p\_RE}}[\mathrm{CycE}][\mathrm{RE}]}{K_{\mathrm{CE}}+[\mathrm{RE}]} + \frac{k_{\mathrm{p\_REE1}}[\mathrm{CycD}][\mathrm{REE1}]}{K_{\mathrm{CD}}+[\mathrm{REE1}]} + \frac{k_{\mathrm{p\_REE1}}[\mathrm{CycE}][\mathrm{REE1}]}{K_{\mathrm{CE}}+[\mathrm{REE1}]} + k_{\mathrm{RpE}}[\mathrm{RB_p}][\mathrm{E2F1}] - D_{\mathrm{RpE}}[\mathrm{R_pE}] - \frac{k_{\mathrm{DP2}}[\mathrm{R_pE}]}{K_{\mathrm{DRpE}}+[\mathrm{R_pE}]} - d_{\mathrm{RpE}}[\mathrm{R_pE}] \quad \text{(S8b)}$$

$$\frac{d[\mathrm{RB}]}{dt} = k_{\mathrm{RB}} + \frac{k_{\mathrm{DP1}}[\mathrm{RB_p}]}{K_{\mathrm{RBp}}+[\mathrm{RB_p}]} - \frac{k_{\mathrm{p\_RB}}[\mathrm{CycD}][\mathrm{RB}]}{K_{\mathrm{CD}}+[\mathrm{RB}]} - \frac{k_{\mathrm{p\_RB}}[\mathrm{CycE}][\mathrm{RB}]}{K_{\mathrm{CE}}+[\mathrm{RB}]} - k_{\mathrm{RE}}[\mathrm{RB}]\left([\mathrm{E2F1}]+[\mathrm{E2Fs}]\right) - k_{\mathrm{RE1}}[\mathrm{RB}][\mathrm{E1A}] - k_{\mathrm{RE1}}[\mathrm{RB}][\mathrm{E1E1}] - d_{\mathrm{RB}}[\mathrm{RB}] \quad \text{(S9b)}$$

$$\frac{d[\mathrm{RB_p}]}{dt} = \frac{k_{\mathrm{p\_RB}}[\mathrm{CycD}][\mathrm{RB}]}{K_{\mathrm{CD}}+[\mathrm{RB}]} + \frac{k_{\mathrm{p\_RB}}[\mathrm{CycE}][\mathrm{RB}]}{K_{\mathrm{CE}}+[\mathrm{RB}]} + \frac{k_{\mathrm{p\_RE1}}[\mathrm{CycD}][\mathrm{RE1}]}{K_{\mathrm{CD}}+[\mathrm{RE1}]} + \frac{k_{\mathrm{p\_RE1}}[\mathrm{CycE}][\mathrm{RE1}]}{K_{\mathrm{CE}}+[\mathrm{RE1}]} + \frac{k_{\mathrm{p\_RE1}}[\mathrm{CycD}][\mathrm{REs}]}{K_{\mathrm{CD}}+[\mathrm{REs}]} + \frac{k_{\mathrm{p\_RE1}}[\mathrm{CycE}][\mathrm{REs}]}{K_{\mathrm{CE}}+[\mathrm{REs}]} + D_{\mathrm{RpE}}[\mathrm{R_pE}] - \frac{k_{\mathrm{DP1}}[\mathrm{RB_p}]}{K_{\mathrm{RBp}}+[\mathrm{RB_p}]} - k_{\mathrm{RpE}}[\mathrm{RB_p}][\mathrm{E2F1}] - k_{\mathrm{RpE}}[\mathrm{RB_p}][\mathrm{E1E1}] - d_{\mathrm{RBp}}[\mathrm{RB_p}] \quad \text{(S10b)}$$

$$\frac{d[\mathrm{ARF}]}{dt} = k_{\mathrm{A\_E}}\left(\frac{\left([\mathrm{E2F1}]+[\mathrm{E2Fs}]\right)^3}{K_{\mathrm{A\_E}}^3+\left([\mathrm{E2F1}]+[\mathrm{E2Fs}]\right)^3}\right) + k_{\mathrm{A\_EE1}}\left(\frac{\left([\mathrm{E1E1}]+[\mathrm{EsE1}]\right)^3}{K_{\mathrm{A\_EE1}}^3+\left([\mathrm{E1E1}]+[\mathrm{EsE1}]\right)^3}\right) + k_{\mathrm{A\_RpE}}\left(\frac{[\mathrm{R_pE}]^3}{K_{\mathrm{A\_RpE}}^3+[\mathrm{R_pE}]^3}\right) + k_{\mathrm{A\_REE1}}\left(\frac{[\mathrm{REE1}]^3}{K_{\mathrm{A\_REE1}}^3+[\mathrm{REE1}]^3}\right) + D_{\mathrm{MpA}}[\mathrm{M_pA}] + D_{\mathrm{MA}}[\mathrm{MA}] - k_{\mathrm{MpA}}[\mathrm{MDM2_p}][\mathrm{ARF}] - k_{\mathrm{MA}}[\mathrm{MDM2}][\mathrm{ARF}] - d_{\mathrm{ARF}}[\mathrm{ARF}] \quad \text{(S11b)}$$

$$\frac{d[\mathrm{E1E1}]}{dt} = k_{\mathrm{EE1}}[\mathrm{E2F1}][\mathrm{E1A}] - k_{\mathrm{RE1}}[\mathrm{RB}][\mathrm{E1E1}] - k_{\mathrm{RpE}}[\mathrm{RB_p}][\mathrm{E1E1}] - D_{\mathrm{EE1}}[\mathrm{E1E1}] - d_{\mathrm{EE1}}[\mathrm{E1E1}] \quad \text{(S12)}$$

$$\frac{d[\mathrm{EsE1}]}{dt} = k_{\mathrm{EE1}}[\mathrm{E2Fs}][\mathrm{E1A}] - D_{\mathrm{EE1}}[\mathrm{EsE1}] - d_{\mathrm{EE1}}[\mathrm{EsE1}] \quad \text{(S13)}$$

$$\frac{d[\mathrm{REE1}]}{dt} = k_{\mathrm{RE1}}[\mathrm{RE}][\mathrm{E1A}] + k_{\mathrm{RE1}}[\mathrm{RB}][\mathrm{E1E1}] + k_{\mathrm{RpE}}[\mathrm{RB_p}][\mathrm{E1E1}] + k_{\mathrm{REE1}}[\mathrm{RE1}][\mathrm{E2F1}] - \frac{k_{\mathrm{p\_REE1}}[\mathrm{CycD}][\mathrm{REE1}]}{K_{\mathrm{CD}}+[\mathrm{REE1}]} - \frac{k_{\mathrm{p\_REE1}}[\mathrm{CycE}][\mathrm{REE1}]}{K_{\mathrm{CE}}+[\mathrm{REE1}]} - D_{\mathrm{REE1}}[\mathrm{REE1}] - d_{\mathrm{REE1}}[\mathrm{REE1}] \quad \text{(S14)}$$

$$\frac{d[\mathrm{RE1}]}{dt} = k_{\mathrm{RE1}}[\mathrm{RB}][\mathrm{E1A}] + k_{\mathrm{RE1}}[\mathrm{REs}][\mathrm{E1A}] + D_{\mathrm{REE1}}[\mathrm{REE1}] - \frac{k_{\mathrm{p\_RE1}}[\mathrm{CycD}][\mathrm{RE1}]}{K_{\mathrm{CD}}+[\mathrm{RE1}]} - \frac{k_{\mathrm{p\_RE1}}[\mathrm{CycE}][\mathrm{RE1}]}{K_{\mathrm{CE}}+[\mathrm{RE1}]} - k_{\mathrm{REE1}}[\mathrm{RE1}][\mathrm{E2F1}] - d_{\mathrm{RE1}}[\mathrm{RE1}] \quad \text{(S15)}$$

$$\frac{d[\mathrm{E1A}]}{dt} = k_{\mathrm{E1A}} + D_{\mathrm{EE1}}\left([\mathrm{E1E1}]+[\mathrm{EsE1}]\right) + \frac{k_{\mathrm{p\_RE1}}[\mathrm{CycD}][\mathrm{RE1}]}{K_{\mathrm{CD}}+[\mathrm{RE1}]} + \frac{k_{\mathrm{p\_RE1}}[\mathrm{CycE}][\mathrm{RE1}]}{K_{\mathrm{CE}}+[\mathrm{RE1}]} + \frac{k_{\mathrm{p\_REE1}}[\mathrm{CycD}][\mathrm{REE1}]}{K_{\mathrm{CD}}+[\mathrm{REE1}]} + \frac{k_{\mathrm{p\_REE1}}[\mathrm{CycE}][\mathrm{REE1}]}{K_{\mathrm{CE}}+[\mathrm{REE1}]} - k_{\mathrm{EE1}}\left([\mathrm{E2F1}]+[\mathrm{E2Fs}]\right)[\mathrm{E1A}] - k_{\mathrm{RE1}}\left([\mathrm{RB}]+[\mathrm{RE}]+[\mathrm{REs}]\right)[\mathrm{E1A}] - d_{\mathrm{E1A}}[\mathrm{E1A}] \quad \text{(S16)}$$

Module 2: p53 activation

$$\frac{d[\mathrm{MDM2}]}{dt} = \frac{k_{\mathrm{MD\_S}}[S]}{K_{\mathrm{MD\_S}}+[S]} + \frac{k_{\mathrm{M\_p}}[\mathrm{p53}]^{n_1}}{K_{\mathrm{M\_p}}^{n_1}+[\mathrm{p53}]^{n_1}} + D_{\mathrm{MA}}[\mathrm{MA}] + \frac{k_{\mathrm{Dp4}}[\mathrm{MDM2_p}]}{K_{\mathrm{Mp}}+[\mathrm{MDM2_p}]} - k_{\mathrm{MA}}[\mathrm{MDM2}][\mathrm{ARF}] - \frac{k_{\mathrm{p\_M}}[\mathrm{Akt}][\mathrm{MDM2}]}{K_{\mathrm{Akt\_M}}+[\mathrm{MDM2}]} - d_{\mathrm{Mdm2}}[\mathrm{MDM2}] \quad \text{(S17)}$$

$$\frac{d[\mathrm{MDM2_p}]}{dt} = D_{\mathrm{MpA}}[\mathrm{M_pA}] + \frac{k_{\mathrm{p\_M}}[\mathrm{Akt}][\mathrm{MDM2}]}{K_{\mathrm{Akt\_M}}+[\mathrm{MDM2}]} - k_{\mathrm{MpA}}[\mathrm{MDM2_p}][\mathrm{ARF}] - \frac{k_{\mathrm{Dp4}}[\mathrm{MDM2_p}]}{K_{\mathrm{Mp}}+[\mathrm{MDM2_p}]} - d_{\mathrm{Mp}}[\mathrm{MDM2_p}] \quad \text{(S18)}$$

$$\frac{d[\mathrm{MA}]}{dt} = k_{\mathrm{MA}}[\mathrm{MDM2}][\mathrm{ARF}] - D_{\mathrm{MA}}[\mathrm{MA}] - d_{\mathrm{MA}}[\mathrm{MA}] \quad \text{(S19)}$$

$$\frac{d[\mathrm{M_pA}]}{dt} = k_{\mathrm{MpA}}[\mathrm{MDM2_p}][\mathrm{ARF}] - D_{\mathrm{MpA}}[\mathrm{M_pA}] - d_{\mathrm{MpA}}[\mathrm{M_pA}] \quad \text{(S20)}$$

$$\frac{d[\mathrm{p53}]}{dt} = k_{\mathrm{p53}} - \frac{k_{\mathrm{M53}}[\mathrm{MDM2}][\mathrm{p53}]}{K_{\mathrm{M53}}+[\mathrm{p53}]} - \frac{k_{\mathrm{Mp53}}[\mathrm{MDM2_p}][\mathrm{p53}]}{K_{\mathrm{Mp53}}+[\mathrm{p53}]} - d_{\mathrm{p53}}[\mathrm{p53}] \quad \text{(S21)}$$

$$\frac{d[\mathrm{PTEN}]}{dt} = k_{\mathrm{PTEN}} + \frac{k_{\mathrm{P\_p}}[\mathrm{p53}]^{n_2}}{K_{\mathrm{P\_p}}^{n_2}+[\mathrm{p53}]^{n_2}} - d_{\mathrm{PTEN}}[\mathrm{PTEN}] \quad \text{(S22)}$$

$$\frac{d[\mathrm{Akt}]}{dt} = \frac{k_{\mathrm{A\_S}}[S]}{K_{\mathrm{A\_S}}+[S]} \frac{[\mathrm{Akt}]_{\mathrm{t}}-[\mathrm{Akt}]}{K_0+[\mathrm{Akt}]_{\mathrm{t}}-[\mathrm{Akt}]} - \frac{k_{\mathrm{DP3}}[\mathrm{Akt}]}{K_{\mathrm{Akt}}+[\mathrm{Akt}]} - \frac{k_{\mathrm{A\_P}}[\mathrm{PTEN}][\mathrm{Akt}]}{K_{\mathrm{AP}}+[\mathrm{Akt}]} \quad \text{(S23)}$$

Module 3: Apoptosis induction mediated by p53 and E2F1

$$\frac{d[\mathrm{Pro\,9}]}{dt} = k_{\mathrm{Pro9}} + k_{\mathrm{C9\_E}}\left(\frac{[\mathrm{E2F1}]}{K_{\mathrm{C9\_E}}+[\mathrm{E2F1}]}\right) + k_{\mathrm{C9\_E}}\left(\frac{[\mathrm{E1E1}]}{K_{\mathrm{C9\_E1E1}}+[\mathrm{E1E1}]}\right) + k_{\mathrm{C9\_E}}\left(\frac{[\mathrm{R_pE}]}{K_{\mathrm{C9\_RpE}}+[\mathrm{R_pE}]}\right) + k_{\mathrm{C9\_E}}\left(\frac{[\mathrm{REE1}]}{K_{\mathrm{C9\_REE1}}+[\mathrm{REE1}]}\right) + D_{\mathrm{AP}}[\mathrm{A\text{-}Pro\,9}] - k_{\mathrm{AP}}[\mathrm{Apop}][\mathrm{Pro\,9}] - k_{\mathrm{A2P}}[\mathrm{A\text{-}Pro\,9}][\mathrm{Pro\,9}] - d_{\mathrm{Pro9}}[\mathrm{Pro\,9}] \quad \text{(S24)}$$

$$\frac{d[\text{Pro 3}]}{dt} = k_{\text{Pro3}} + k_{\text{C3\_E}}\left(\frac{[\text{E2F1}]}{K_{\text{C3\_E}} + [\text{E2F1}]}\right) + k_{\text{C3\_E}}\left(\frac{[\text{E1E1}]}{K_{\text{C3\_E1E1}} + [\text{E1E1}]}\right) + k_{\text{C3\_E}}\left(\frac{[\text{R}_\text{p}\text{E}]}{K_{\text{C3\_RpE}} + [\text{R}_\text{p}\text{E}]}\right) + k_{\text{C3\_E}}\left(\frac{[\text{REE1}]}{K_{\text{C3\_REE1}} + [\text{REE1}]}\right) + D_{\text{21P}}[\text{p21}_\text{p} - \text{Pro 3}] - \frac{k_{\text{AC9}}[\text{A-Casp 9}][\text{Pro 3}]^{n_5}}{K_{\text{AC9}}^{n_5} + [\text{Pro 3}]^{n_5}} - \frac{k_{\text{C9}}[\text{Casp 9}][\text{Pro 3}]^{n_5}}{K_{\text{C9}}^{n_5} + [\text{Pro 3}]^{n_5}} - k_{\text{21P}}[\text{p21}_\text{p}][\text{Pro 3}] - d_{\text{Pro3}}[\text{Pro 3}] \tag{S25}$$

$$\frac{d[\text{Apaf-1}]}{dt} = k_{\text{Apaf1}} + k_{\text{Af\_E}}\left(\frac{[\text{E2F1}]}{K_{\text{Af\_E}} + [\text{E2F1}]}\right) + k_{\text{Af\_E}}\left(\frac{[\text{E1E1}]}{K_{\text{Af\_E1E1}} + [\text{E1E1}]}\right) + k_{\text{Af\_E}}\left(\frac{[\text{R}_\text{p}\text{E}]}{K_{\text{Af\_RpE}} + [\text{R}_\text{p}\text{E}]}\right) + k_{\text{Af\_E}}\left(\frac{[\text{REE1}]}{K_{\text{Af\_REE1}} + [\text{REE1}]}\right) + D_{\text{CA}}[\text{C-Apaf1}] - k_{\text{CA}}[\text{Cytc}][\text{Apaf-1}] - d_{\text{Apaf1}}[\text{Apaf-1}] \tag{S26}$$

$$\frac{d[\text{p21}]}{dt} = k_{\text{p21}} + \frac{k_{\text{21\_p}}[\text{p53}]^3}{K_{\text{21\_p}}^3 + [\text{p53}]^3} + \frac{k_{\text{DP5}}[\text{p21}_\text{p}]}{K_{\text{p21p}} + [\text{p21}_\text{p}]} - \frac{k_{\text{p\_21}}[\text{Akt}][\text{p21}]}{K_{\text{Akt\_p21}} + [\text{p21}]} - \frac{k_{\text{C3}}[\text{Casp3}][\text{p21}]}{K_{\text{C3}} + [\text{p21}]} - d_{\text{21}}[\text{p21}] \tag{S27}$$

$$\frac{d[\text{p21}_\text{p}]}{dt} = D_{\text{21P}}[\text{p21}_\text{p}\text{-Pro3}] + \frac{k_{\text{p\_21}}[\text{Akt}][\text{p21}]}{K_{\text{Akt\_p21}} + [\text{p21}]} - k_{\text{21P}}[\text{p21}_\text{p}][\text{Pro3}] - \frac{k_{\text{DP5}}[\text{p21}_\text{p}]}{K_{\text{p21p}} + [\text{p21}_\text{p}]} - \frac{k_{\text{C3}}[\text{Casp3}][\text{p21}_\text{p}]}{K_{\text{C3}} + [\text{p21}_\text{p}]} - d_{\text{21p}}[\text{p21}_\text{p}] \tag{S28}$$

$$\frac{d[\text{Bax}]}{dt} = k_{\text{Bax}} + \frac{k_{\text{B\_p}}[\text{p53}]^{n_3}}{K_{\text{B\_p}}^{n_3} + [\text{p53}]^{n_3}} - d_{\text{Bax}}[\text{Bax}] \tag{S29}$$

$$\frac{d[\text{Cytc}]}{dt} = \left(k_{\text{Cytc}} + k_{\text{C\_B}}[\text{Bax}] + \frac{k_{\text{C\_C3}}[\text{Casp3}]^{n_6}}{K_{\text{C\_C3}}^{n_6} + [\text{Casp3}]^{n_6}}\right)[\text{Cytc}_\text{m}] + D_{\text{CA}}[\text{C-Apaf1}] - k_{\text{CA}}[\text{Cytc}][\text{Apaf-1}] - d_{\text{Cytc}}[\text{Cytc}] \tag{S30}$$

$$[\text{Cytc}_\text{c}] = [\text{Cytc}] + [\text{C-Apaf1}] + 7([\text{Apop}] + [\text{A-Pro9}] + [\text{A-Casp9}])$$

$$[\text{Cytc}_\text{m}] = \text{Cytc}_{\text{free}}\text{Cytc}_\text{t} + \text{Cytc}_{\text{bound}}\text{Cytc}_\text{t}\frac{[\text{Casp3}]^{n_4}}{K_{\text{Ct\_C3}}^{n_4} + [\text{Casp3}]^{n_4}} - [\text{Cytc}_\text{c}]$$

$$\frac{d[\text{C-Apaf1}]}{dt} = k_{\text{CA}}[\text{Cytc}][\text{Apaf-1}] - D_{\text{CA}}[\text{C-Apaf1}] - 7k_{\text{Apop}}[\text{C-Apaf1}]^4 - d_{\text{C-A}}[\text{C-Apaf1}] \tag{S31}$$

$$\frac{d[\text{Apop}]}{dt} = k_{\text{Apop}}[\text{C-Apaf1}]^4 + D_{\text{AP}}[\text{A-Pro 9}] + D_{\text{A2C}}[\text{A-Casp 9}] - k_{\text{AP}}[\text{Apop}][\text{Pro 9}] - k_{\text{A2C}}[\text{Apop}][\text{Casp 9}] - d_{\text{Apop}}[\text{Apop}] \tag{S32}$$

$$\frac{d[\text{A-Pro9}]}{dt} = k_{\text{AP}}[\text{Apop}][\text{Pro9}] - k_{\text{A2P}}[\text{A-Pro9}][\text{Pro9}] - D_{\text{AP}}[\text{A-Pro9}] \tag{S33}$$

$$\frac{d[\text{A-Casp9}]}{dt} = k_{\text{A2P}}[\text{A-Pro9}][\text{Pro9}] + k_{\text{A2C}}[\text{Apop}][\text{Casp9}] - D_{\text{A2C}}[\text{A-Casp9}] \tag{S34}$$

$$\frac{d[\text{Casp9}]}{dt} = D_{\text{A2C}}[\text{A-Casp9}] - k_{\text{A2C}}[\text{Apop}][\text{Casp9}] - d_{\text{C9}}[\text{Casp9}] \tag{S35}$$

$$\frac{d[\text{Casp3}]}{dt} = \frac{k_{\text{AC9}}[\text{A-Casp9}][\text{Pro3}]^{n_5}}{K_{\text{AC9}}^{n_5} + [\text{Pro3}]^{n_5}} + \frac{k_{\text{C9}}[\text{Casp9}][\text{Pro3}]^{n_5}}{K_{\text{C9}}^{n_5} + [\text{Pro3}]^{n_5}} - d_{\text{C3}}[\text{Casp3}] \tag{S36}$$

$$\frac{d[\text{p21}_\text{p}\text{-Pro3}]}{dt} = k_{\text{21P}}[\text{p21}_\text{p}][\text{Pro3}] - D_{\text{21P}}[\text{p21}_\text{p}\text{-Pro3}] - d_{\text{21P}}[\text{p21}_\text{p}\text{-Pro3}] \tag{S37}$$

II. SI Appendix Tables

Table S1： All species in the model

In most cases, the initial levels of all proteins are based on their steady-state levels at 10% serum without E1A.

Variable	Meaning and interpretation	Initial value
Species in module 1		
S	serum concentration; it is proportional to the concentration of GFs; GFs induce mitogenic signals	serum-rich: 10% serum-free: 0.1%
Myc	Myc protein	1.21 (0)
CycD	active cyclin D-Cdk4/6 complex	0.43 (0)
CycE	active cyclin E-Cdk2 complex	0.50 (0)
E2F1	transcription factor E2F1	0.28 (0)
E2Fs	E2F2 and E2F3A	0.63 (0)
RE	RB-E2F1 complex	0.29 (0.65)
REs	RB-E2Fs complex	0.36 (0.8)
R_pE	RB_p-E2F1 complex, keeping the transcriptional activity as free E2F1 while being more resistant to degradation than E2F1	0.61 (0)
RB	RB protein	0.021 (1.5)
RB_p	phosphorylated form of RB	1.03 (0)
ARF	free ARF protein ($p14^{ARF}$)	0.03 (0)
E1E1	E2F1-E1A complex	0
EsE1	E2Fs-E1A complex	0
REE1	RB-E2F1-E1A complex, keeping the transcriptional activity as free E2F1 while being more resistant to degradation than E2F1	0
RE1	RB-E1A complex	0
E1A	adenoviral E1A protein	0
Species in module 2		
MDM2	MDM2 is evenly distributed in the nucleus and cytosol	0.2
$MDM2_p$	phosphorylated MDM2, which is mainly distributed in the nucleus	4.76

MA	MDM2-ARF complex	0.038
M_pA	$MDM2_p$-ARF complex	0.058
p53	p53 in the nucleus	0.006
PTEN	p53 target, inhibiting Akt activation by dephosphorylating PIP3	0.1
Akt	active Akt	0.78
Akt_t	total amount of Akt, which is much more than active Akt and is considered a constant	2.5
Species in module 3		
Pro9	procaspase-9	0.51
Pro3	procaspase-3	0.42
Apaf-1	one of key components making up the apoptosome	0.66
p21	p53 target, which mainly resides in the nucleus	0.005
$p21_p$	phosphorylated p21, which is evenly distributed in the nucleus and cytosol	0.029
Bax	active form of Bax (Bax oligomers)	0
Cytc	free Cyt *c* in the cytosol	0
$Cytc_c$	total Cyt *c* in the cytosol, comprising Cyt *c*, C-Apaf1, Apop, A-Pro9 and A-Casp9	--
$Cytc_m$	free and soluble Cyt *c* in mitochondria, which is ready for release as long as there are pores on the outer membrane of mitochondria	--
$Cytc_t$	total amount of Cyt *c* within the cell, which is assumed to be a constant	2.0 (constant)
$Cytc_{free}$	ratio of free Cyt *c* to total amount of Cyt *c* in mitochondria	0.14 (constant)
$Cytc_{bound}$	ratio of bound Cyt *c* to total amount of Cyt *c* in mitochondria	0.86 (constant)
C-Apaf1	Cyt *c*-Apaf-1 heterodimer	0
Apop	Apoptosome; the main foci for the activation of caspase-9 and caspase-3	0
A-Pro9	the complex comprising one apoptosome and one procaspase-9	0

A-Casp9	the complex comprising one apoptosome and two active caspase-9; it is much more efficient than free caspase-9 in catalyzing the activation of caspase-3	0
Casp9	free caspase-9 dimer, which keeps the activity of catalyzing the cleavage and activation of caspase-3	0
Casp3	proteolytically active caspase-3 dimer	0
$p21_p$-Pro3	the complex of phosphorylated p21 and procaspase-3	0.17

The numbers in parentheses denote the initial values used in plotting Figs. 2*C*, S2*B* and S2*C* (serum-free, without E1A). Such a setting is to follow the experimental protocol in Ref. 1.

Table S2: Reaction kinetics in the model

Reaction	Kinetic equation
Synthesis of species	
$*\xrightarrow{\text{S, E, EE1, RpE, REE1}}\text{Myc}$ (E:E2F1+E2Fs, EE1:E1E1+EsE1)	$\frac{k_{\text{M\_S}}[S]}{K_{\text{S}}+[S]}+k_{\text{M\_E}}\left(\frac{[\text{E}]}{K_{\text{E}}+[\text{E}]}\right)+k_{\text{M\_E}}\left(\frac{[\text{EE1}]}{K_{\text{EE1}}+[\text{EE1}]}\right)+k_{\text{M\_E}}\left(\frac{[\text{R}_\text{p}\text{E}]}{K_{\text{RpE}}+[\text{R}_\text{p}\text{E}]}\right)+k_{\text{M\_E}}\left(\frac{[\text{REE1}]}{K_{\text{REE1}}+[\text{REE1}]}\right)$
$*\xrightarrow{\text{S, Myc}}\text{CycD}$	$\frac{k_{\text{CD\_S}}[S]}{K_{\text{S}}+[S]}+\frac{k_{\text{CD\_M}}[\text{Myc}]}{K_{\text{M}}+[\text{Myc}]}$
$*\xrightarrow{\text{E, EE1, RpE, REE1}}\text{CycE}$ (E:E2F1+E2Fs, EE1:E1E1+EsE1)	$k_{\text{CE\_E}}\left(\frac{[\text{E}]}{K_{\text{E}}+[\text{E}]}\right)+k_{\text{CE\_E}}\left(\frac{[\text{EE1}]}{K_{\text{EE1}}+[\text{EE1}]}\right)+k_{\text{CE\_E}}\left(\frac{[\text{R}_\text{p}\text{E}]}{K_{\text{RpE}}+[\text{R}_\text{p}\text{E}]}\right)+k_{\text{CE\_E}}\left(\frac{[\text{REE1}]}{K_{\text{REE1}}+[\text{REE1}]}\right)$
$*\longrightarrow\text{E2F}$	k_{E2F}
$*\xrightarrow{\text{Myc, E, EE1, RpE, REE1}}\text{E2F}$ (E:E2F1+E2Fs, EE1:E1E1+EsE1)	$\frac{k_{\text{E\_M}}[\text{Myc}]}{K_{\text{M}}+[\text{Myc}]}+k_{\text{E\_E}}\left(\frac{[\text{Myc}]}{K_{\text{M}}+[\text{Myc}]}\right)\left(\frac{[\text{E}]}{K_{\text{E}}+[\text{E}]}\right)+k_{\text{E\_E}}\left(\frac{[\text{Myc}]}{K_{\text{M}}+[\text{Myc}]}\right)\left(\frac{[\text{EE1}]}{K_{\text{EE1}}+[\text{EE1}]}\right)+k_{\text{E\_E}}\left(\frac{[\text{Myc}]}{K_{\text{M}}+[\text{Myc}]}\right)\left(\frac{[\text{R}_\text{p}\text{E}]}{K_{\text{RpE}}+[\text{R}_\text{p}\text{E}]}\right)+k_{\text{E\_E}}\left(\frac{[\text{Myc}]}{K_{\text{M}}+[\text{Myc}]}\right)\left(\frac{[\text{REE1}]}{K_{\text{REE1}}+[\text{REE1}]}\right)$
$*\xrightarrow{\text{E, EE1, RpE, REE1}}\text{ARF}$ (E:E2F1+E2Fs, EE1:E1E1+EsE1)	$k_{\text{A\_E}}\left(\frac{[\text{E}]^3}{K_{\text{A\_E}}^3+[\text{E}]^3}\right)+k_{\text{A\_EE1}}\left(\frac{[\text{EE1}]^3}{K_{\text{A\_EE1}}^3+[\text{EE1}]^3}\right)+k_{\text{A\_RpE}}\left(\frac{[\text{R}_\text{p}\text{E}]^3}{K_{\text{A\_RpE}}^3+[\text{R}_\text{p}\text{E}]^3}\right)+k_{\text{A\_REE1}}\left(\frac{[\text{REE1}]^3}{K_{\text{A\_REE1}}^3+[\text{REE1}]^3}\right)$
$*\xrightarrow{\text{p53}}\text{MDM2}$	$\frac{k_{\text{M\_p}}[\text{p53}]^{n_1}}{K_{\text{M\_p}}^{n_1}+[\text{p53}]^{n_1}}$
$*\xrightarrow{\text{S}}\text{MDM2}$	$\frac{k_{\text{MD\_S}}[S]}{K_{\text{MD\_S}}+[S]}$

$*\xrightarrow{\text{p53}}\text{PTEN}$	$\frac{k_{\text{P\_p}}[\text{p53}]^{n_2}}{K_{\text{P\_p}}^{n_2}+[\text{p53}]^{n_2}}$
$*\longrightarrow\text{PTEN}$	k_{PTEN}
$*\longrightarrow\text{E1A}$	k_{E1A}
$*\longrightarrow\text{RB}$	k_{RB}
$*\longrightarrow\text{p53}$	k_{p53}
$*\xrightarrow{\text{E2F1, E1E1, R}_\text{p}\text{E, REE1}}\text{Pro9}$	$k_{\text{C9\_E}}\left(\frac{[\text{E2F1}]}{K_{\text{C9\_E}}+[\text{E2F1}]}\right)+k_{\text{C9\_E}}\left(\frac{[\text{E1E1}]}{K_{\text{C9\_E1E1}}+[\text{E1E1}]}\right)+k_{\text{C9\_E}}\left(\frac{[\text{R}_\text{p}\text{E}]}{K_{\text{C9\_RpE}}+[\text{R}_\text{p}\text{E}]}\right)+k_{\text{C9\_E}}\left(\frac{[\text{REE1}]}{K_{\text{C9\_REE1}}+[\text{REE1}]}\right)$
$*\longrightarrow\text{Pro9}$	k_{Pro9}
$*\xrightarrow{\text{E2F1, E1E1, R}_\text{p}\text{E, REE1}}\text{Pro3}$	$k_{\text{C3\_E}}\left(\frac{[\text{E2F1}]}{K_{\text{C3\_E}}+[\text{E2F1}]}\right)+k_{\text{C3\_E}}\left(\frac{[\text{E1E1}]}{K_{\text{C3\_E1E1}}+[\text{E1E1}]}\right)+k_{\text{C3\_E}}\left(\frac{[\text{R}_\text{p}\text{E}]}{K_{\text{C3\_RpE}}+[\text{R}_\text{p}\text{E}]}\right)+k_{\text{C3\_E}}\left(\frac{[\text{REE1}]}{K_{\text{C3\_REE1}}+[\text{REE1}]}\right)$
$*\longrightarrow\text{Pro3}$	k_{Pro3}
$*\xrightarrow{\text{E2F1, E1E1, R}_\text{p}\text{E, REE1}}\text{Apaf1}$	$k_{\text{Af\_E}}\left(\frac{[\text{E2F1}]}{K_{\text{Af\_E}}+[\text{E2F1}]}\right)+k_{\text{Af\_E}}\left(\frac{[\text{E1E1}]}{K_{\text{Af\_E1E1}}+[\text{E1E1}]}\right)+k_{\text{Af\_E}}\left(\frac{[\text{R}_\text{p}\text{E}]}{K_{\text{Af\_RpE}}+[\text{R}_\text{p}\text{E}]}\right)+k_{\text{Af\_E}}\left(\frac{[\text{REE1}]}{K_{\text{Af\_REE1}}+[\text{REE1}]}\right)$
$*\longrightarrow\text{Apaf-1}$	k_{Apaf1}
$*\xrightarrow{\text{p53}}\text{p21}$	$\frac{k_{21\_\text{p}}[\text{p53}]^3}{K_{21\_\text{p}}^3+[\text{p53}]^3}$
$*\longrightarrow\text{p21}$	k_{p21}
$*\xrightarrow{\text{p53}}\text{Bax}$	$\frac{k_{\text{B\_p}}[\text{p53}]^{n_3}}{K_{\text{B\_p}}^{n_3}+[\text{p53}]^{n_3}}$
$*\longrightarrow\text{Bax}$	k_{Bax}
$*\xrightarrow{\text{Bax}}\text{Cytc}$	$k_{\text{C\_B}}[\text{Bax}][\text{Cytc}_\text{m}]$

$*\xrightarrow{\text{Casp3}}\text{Cytc}$	$\frac{k_{\text{C\_C3}}[\text{Casp3}]^{n_6}}{K_{\text{C\_C3}}^{n_6}+[\text{Casp3}]^{n_6}}[\text{Cytc}_{\text{m}}]$
$*\xrightarrow{\text{Casp3}}\text{Cytc}_{\text{m}}$	$\text{Cytc}_{\text{bound}}\text{Cytc}_{\text{t}}\frac{[\text{Casp3}]^{n_4}}{K_{\text{Ct\_C3}}^{n_4}+[\text{Casp3}]^{n_4}}$
$*\longrightarrow\text{Cytc}$	$k_{\text{Cytc}}[\text{Cytc}_{\text{m}}]$
Complex formation and disassociation	
$\text{RB+E2F1/E2Fs}\longrightarrow\text{RE/REs}$	$k_{\text{RE}}[\text{RB}][\text{E2F1}]$, $k_{\text{RE}}[\text{RB}][\text{E2Fs}]$
$\text{RB}_{\text{p}}+\text{E2F1}\longleftrightarrow\text{R}_{\text{p}}\text{E}$	$k_{\text{RpE}}[\text{RB}_{\text{p}}][\text{E2F1}]$; $D_{\text{RpE}}[\text{R}_{\text{p}}\text{E}]$
$\text{E2F1+E1A}\longleftrightarrow\text{E1E1}$ $\text{E2Fs+E1A}\longleftrightarrow\text{EsE1}$	$k_{\text{EE1}}[\text{E2F1}][\text{E1A}], D_{\text{EE1}}[\text{E1E1}]$; $k_{\text{EE1}}[\text{E2Fs}][\text{E1A}], D_{\text{EE1}}[\text{EsE1}]$
$\text{RB+E1A}\longrightarrow\text{RE1}$	$k_{\text{RE1}}[\text{RB}][\text{E1A}]$
$\text{RE+E1A}\longrightarrow\text{REE1}$	$k_{\text{RE1}}[\text{RE}][\text{E1A}]$
$\text{REs+E1A}\longrightarrow\text{RE1+E2Fs}$	$k_{\text{RE1}}[\text{REs}][\text{E1A}]$
$\text{RB+E1E1}\longrightarrow\text{REE1}$	$k_{\text{RE1}}[\text{RB}][\text{E1E1}]$
$\text{RB}_{\text{p}}+\text{E1E1}\longrightarrow\text{REE1}$	$k_{\text{RpE}}[\text{RB}_{\text{p}}][\text{E1E1}]$
$\text{RE1+E2F1}\longrightarrow\text{REE1}$	$k_{\text{REE1}}[\text{RE1}][\text{E2F1}]$
$\text{MDM2}_{\text{p}}+\text{ARF}\longleftrightarrow\text{M}_{\text{p}}\text{A}$	$k_{\text{MpA}}[\text{MDM2}_{\text{p}}][\text{ARF}]$ $D_{\text{MpA}}[\text{M}_{\text{p}}\text{A}]$
$\text{MDM2+ARF}\longleftrightarrow\text{MA}$	$k_{\text{MA}}[\text{MDM2}][\text{ARF}]$ $D_{\text{MA}}[\text{MA}]$
$\text{REE1}\longrightarrow\text{RE1+E2F1}$	$D_{\text{REE1}}[\text{REE1}]$
$\text{Cytc+Apaf1}\longleftrightarrow\text{C-Apaf1}$	$k_{\text{CA}}[\text{Cytc}][\text{Apaf-1}]$ $D_{\text{CA}}[\text{C-Apaf1}]$
$\text{7C-Apaf1}\longrightarrow\text{Apop}$	$k_{\text{Apop}}[\text{C-Apaf1}]^4$
$\text{p21}_{\text{p}}+\text{Pro3}\longleftrightarrow\text{p21}_{\text{p}}\text{-Pro3}$	$k_{\text{21P}}[\text{p21}_{\text{p}}][\text{Pro3}]$ $D_{\text{21P}}[\text{p21}_{\text{p}}\text{-Pro3}]$
Protein phosphorylation	
$\text{RB}\xrightarrow{\text{CycD, CycE}}\text{RB}_{\text{p}}$	$\frac{k_{\text{p\_RB}}[\text{CycD}][\text{RB}]}{K_{\text{CD}}+[\text{RB}]}+\frac{k_{\text{p\_RB}}[\text{CycE}][\text{RB}]}{K_{\text{CE}}+[\text{RB}]}$

$\mathrm{RE} \xrightarrow{\text{CycD, CycE}} \mathrm{R_pE}$	$\frac{k_{\mathrm{p\_RE}}[\mathrm{CycD}][\mathrm{RE}]}{K_{\mathrm{CD}}+[\mathrm{RE}]}+\frac{k_{\mathrm{p\_RE}}[\mathrm{CycE}][\mathrm{RE}]}{K_{\mathrm{CE}}+[\mathrm{RE}]}$
$\mathrm{REs} \xrightarrow{\text{CycD, CycE}} \mathrm{RB_p+E2Fs}$	$\frac{k_{\mathrm{p\_RE}}[\mathrm{CycD}][\mathrm{REs}]}{K_{\mathrm{CD}}+[\mathrm{REs}]}+\frac{k_{\mathrm{p\_RE}}[\mathrm{CycE}][\mathrm{REs}]}{K_{\mathrm{CE}}+[\mathrm{REs}]}$
$\mathrm{RE1} \xrightarrow{\text{CycD, CycE}} \mathrm{RB_p+E1A}$	$\frac{k_{\mathrm{p\_RE1}}[\mathrm{CycD}][\mathrm{RE1}]}{K_{\mathrm{CD}}+[\mathrm{RE1}]}+\frac{k_{\mathrm{p\_RE1}}[\mathrm{CycE}][\mathrm{RE1}]}{K_{\mathrm{CE}}+[\mathrm{RE1}]}$
$\mathrm{REE1} \xrightarrow{\text{CycD, CycE}} \mathrm{R_pE+E1A}$	$\frac{k_{\mathrm{p\_REE1}}[\mathrm{CycD}][\mathrm{REE1}]}{K_{\mathrm{CD}}+[\mathrm{REE1}]}+\frac{k_{\mathrm{p\_REE1}}[\mathrm{CycE}][\mathrm{REE1}]}{K_{\mathrm{CE}}+[\mathrm{REE1}]}$
$\mathrm{Akt_u} \xrightarrow{\mathrm{S}} \mathrm{Akt}$	$\frac{k_{\mathrm{A\_S}}[S]}{K_{\mathrm{A\_S}}+[S]}\frac{[\mathrm{Akt}]_t-[\mathrm{Akt}]}{K_0+[\mathrm{Akt}]_t-[\mathrm{Akt}]}$
$\mathrm{MDM2} \xrightarrow{\mathrm{Akt}} \mathrm{MDM2_p}$	$\frac{k_{\mathrm{p\_M}}[\mathrm{Akt}][\mathrm{MDM2}]}{K_{\mathrm{Akt\_M}}+[\mathrm{MDM2}]}$
$\mathrm{p21} \xrightarrow{\mathrm{Akt}} \mathrm{p21_p}$	$\frac{k_{\mathrm{p\_21}}[\mathrm{Akt}][\mathrm{p21}]}{K_{\mathrm{Akt\_p21}}+[\mathrm{p21}]}$
Protein dephosphorylation	
$\mathrm{RB_p} \longrightarrow \mathrm{RB}$	$\frac{k_{\mathrm{DP1}}[\mathrm{RB_p}]}{K_{\mathrm{RBp}}+[\mathrm{RB_p}]}$
$\mathrm{R_pE} \longrightarrow \mathrm{RE}$	$\frac{k_{\mathrm{DP2}}[\mathrm{R_pE}]}{K_{\mathrm{DRpE}}+[\mathrm{R_pE}]}$
$\mathrm{Akt} \longrightarrow \mathrm{Akt_u}$	$\frac{k_{\mathrm{DP3}}[\mathrm{Akt}]}{K_{\mathrm{Akt}}+[\mathrm{Akt}]}$
$\mathrm{Akt} \xrightarrow{\mathrm{PTEN}} \mathrm{Akt_u}$	$\frac{k_{\mathrm{A\_P}}[\mathrm{PTEN}][\mathrm{Akt}]}{K_{\mathrm{AP}}+[\mathrm{Akt}]}$
$\mathrm{MDM2_p} \longrightarrow \mathrm{MDM2}$	$\frac{k_{\mathrm{DP4}}[\mathrm{MDM2_p}]}{K_{\mathrm{Mp}}+[\mathrm{MDM2_p}]}$
$\mathrm{p21_p} \longrightarrow \mathrm{p21}$	$\frac{k_{\mathrm{DP5}}[\mathrm{p21_p}]}{K_{\mathrm{p21p}}+[\mathrm{p21_p}]}$
Caspase cascade	
$\mathrm{Apop+Pro9} \longleftrightarrow \mathrm{A\text{-}Pro9}$	$k_{\mathrm{AP}}[\mathrm{Apop}][\mathrm{Pro9}]$ $D_{\mathrm{AP}}[\mathrm{A\text{-}Pro9}]$

A-Pro9+Pro9 $\longrightarrow$ A-Casp9	$k_{A2P}[\text{A-Pro9}][\text{Pro9}]$
Apop+Casp9 $\longleftrightarrow$ A-Casp9	$k_{A2C}[\text{Apop}][\text{Casp9}]$ $D_{A2C}[\text{A-Casp9}]$
Pro3 $\xrightarrow{\text{A-Casp9，Casp9}}$ Casp3	$\frac{k_{AC9}[\text{A-Casp9}][\text{Pro3}]^{n_5}}{K_{AC9}^{n_5}+[\text{Pro3}]^{n_5}}+\frac{k_{C9}[\text{Casp9}][\text{Pro3}]^{n_5}}{K_{C9}^{n_5}+[\text{Pro3}]^{n_5}}$
Degradation of different species	
Myc $\longrightarrow$ * CycD $\longrightarrow$ *,CycE $\longrightarrow$ * E2F1, E2Fs $\longrightarrow$ * RE, REs $\longrightarrow$ * $R_pE \longrightarrow$ * E1E1, EsE1 $\longrightarrow$ * REE1 $\longrightarrow$ * RB $\longrightarrow$ *, $RB_p \longrightarrow$ * RE1 $\longrightarrow$ * ARF $\longrightarrow$ * MDM2 $\longrightarrow$ *, $MDM2_p \longrightarrow$ * MA $\longrightarrow$ *, $M_pA \longrightarrow$ * E1A $\longrightarrow$ * PTEN $\longrightarrow$ * p53 $\longrightarrow$ * p53 $\xrightarrow{\text{MDM2}}$ *, p53 $\xrightarrow{\text{MDM2p}}$ * p21 $\longrightarrow$ *, $p21_p \longrightarrow$ * $p21_p$-Pro3 $\longrightarrow$ * $p21_p \xrightarrow{\text{Casp3}}$ *, p21 $\xrightarrow{\text{Casp3}}$ * Bax $\longrightarrow$ * Cytc $\longrightarrow$ *, Apaf-1 $\longrightarrow$ * C-Apaf1 $\longrightarrow$ *, Apop $\longrightarrow$ * Pro9 $\longrightarrow$ *, Casp9 $\longrightarrow$ * Pro3 $\longrightarrow$ *, Casp3 $\longrightarrow$ *	$d_{Myc}[\text{Myc}]$ $d_{CD}[\text{CycD}], d_{CE}[\text{CycE}]$ $d_{E2F}[\text{E2F1}], d_{E2F}[\text{E2Fs}]$ $d_{RE}[\text{RE}], d_{RE}[\text{REs}]$ $d_{RpE}[R_pE]$ $d_{EE1}[\text{E1E1}], d_{EE1}[\text{EsE1}]$ $d_{REE1}[\text{REE1}]$ $d_{RB}[\text{RB}], d_{RBp}[RB_p]$ $d_{RE1}[\text{RE1}]$ $d_{ARF}[\text{ARF}]$ $d_{Mdm2}[\text{MDM2}], d_{Mp}[MDM2_p]$ $d_{MA}[\text{MA}], d_{MpA}[M_pA]$ $d_{E1A}[\text{E1A}]$ $d_{PTEN}[\text{PTEN}]$ $d_{p53}[\text{p53}]$ $\frac{k_{M53}[\text{MDM2}][\text{p53}]}{K_{M53}+[\text{p53}]}, \frac{k_{Mp53}[MDM2_p][\text{p53}]}{K_{Mp53}+[\text{p53}]}$ $d_{21}[\text{p21}], d_{21p}[p21_p]$ $d_{21P}[p21_p-\text{Pro3}]$ $\frac{k_{C3}[\text{Casp3}][p21_p]}{K_{C3}+[p21_p]}, \frac{k_{C3}[\text{Casp3}][\text{p21}]}{K_{C3}+[\text{p21}]}$ $d_{Bax}[\text{Bax}]$ $d_{Cytc}[\text{Cytc}], d_{Apaf1}[\text{Apaf-1}]$ $d_{C\text{-}A}[\text{C-Apaf1}], d_{Apop}[\text{Apop}]$ $d_{Pro9}[\text{Pro9}], d_{C9}[\text{Casp9}]$ $d_{Pro3}[\text{Pro3}], d_{C3}[\text{Casp3}]$

Table S3: Standard parameter values of the model

Parameter	Value	Interpretation
Synthesis of species		
k_{M_S}	0.6 μM/h	Rate constant of Myc expression induced by serum; adapted from Ref.1
k_{M_E}	0.1 μM/h	Rate constant of E2F-mediated expression of Myc
k_{CD_S}	0.5 μM/h	Rate constant of cyclin D expression induced by serum
k_{CD_M}	0.11 μM/h	Rate constant of Myc-mediated expression of cyclin D
k_{CE_E}	0.35 μM/h	Rate constant of E2F-mediated expression of cyclin E; adapted from Ref. 1
k_{E2F}	0.005 μM/h	Basal rate constant of E2F expression
k_{E_M}	0.001 μM/h	Rate constant of Myc-mediated expression of E2F; adapted from Ref. 1
k_{E_E}	0.15 μM/h	Rate constant of E2F-mediated expression of E2F; adapted from Ref.1
k_{A_E}	0.25 μM/h	Rate constant of E2F-mediated expression of ARF
k_{A_EE1}	0.5 μM/h	Rate constant of ARF expression mediated by the E2F-E1A complex
k_{A_RpE}	0.25 μM/h	Rate constant of ARF expression mediated by the RB_p-E2F1 complex
k_{A_REE1}	0.5 μM/h	Rate constant of ARF expression mediated by the RB-E2F1-E1A complex
k_{MD_S}	0.66 μM/h	Rate constant of MDM2 expression induced by serum; it is nearly twice the degradation rate of MDM2[72]
k_{M_p}	0.33 μM/h	Rate constant of p53-mediated expression of MDM2
n_1	4	Hill coefficient of p53-dependent expression of MDM2
k_{P_p}	0.7 μM/h	Rate constant of p53-dependent synthesis of PTEN[11]
n_2	3	Hill coefficient of p53-dependent synthesis of PTEN
k_{PTEN}	0.05 μM/h	Basal expression rate of PTEN
k_{E1A}	0.8 μM/h	Basal rate constant of E1A expression
k_{RB}	0.18 μM/h	Basal rate constant of RB expression; adapted from Ref. 1
k_{p53}	4.8 μM/h	Basal rate constant of p53 expression, estimated at 0.005~0.2 μM/min[72]
k_{C9_E}	0.1 μM/h	Rate constant of E2F1-induced expression of procaspase-9
k_{Pro9}	0.01 μM/h	Basal rate constant of procaspase-9 expression
k_{C3_E}	0.15 μM/h	Rate constant of E2F1-induced procaspase-3 expression
k_{Pro3}	0.01 μM/h	Basal rate constant of procaspase-3 expression

$k_{\mathrm{Af\_E}}$	0.55 μM/h	Rate constant of E2F1-induced Apaf-1expression
k_{Apaf1}	0.055 μM/h	Basal rate constant of Apaf-1expression
$k_{\mathrm{21\_p}}$	1.2 μM/h	Rate constant of p53-induced p21 expression
k_{p21}	0.1 μM/h	Basal rate constant of p21 expression
$k_{\mathrm{B\_p}}$	0.1 μM/h	Rate constant of p53-induced expression and activation of Bax
n_3	3	Hill coefficient of p53-induced expression and activation of Bax
k_{Bax}	0 μM/h	Basal activation rate of Bax
K_{S}	0.5%	Michaelis constant for transcription of cell-cycle regulators (e.g. Myc, cyclin D) triggered by growth factors; adapted from Ref. 1
$K_{\mathrm{MD\_S}}$	0.45%	Michaelis constant for MDM2 expression triggered by growth factors
K_{M}	0.5 μM	Michaelis constant for Myc-mediated expression of target genes (e.g. cyclin D and E2F)
K_{E}	0.2 μM	Michaelis constant for E2F-mediated expression of target genes (e.g. Myc, Cyclin E and E2F)
$K_{\mathrm{A\_E}}$	1.3 μM	Hill constant for E2F-mediated expression of ARF; it is assumed to be significantly greater than K_{E}
$K_{\mathrm{C9\_E}}$	0.7 μM	Michaelis constant for E2F-mediated expression of procaspase-9
$K_{\mathrm{C3\_E}}$	0.5 μM	Michaelis constant for E2F-mediated expression of procaspase-3
$K_{\mathrm{Af\_E}}$	0.5 μM	Michaelis constant for E2F-mediated expression of Apaf-1
K_{EE1}	0.2 μM	Michaelis constant for E2F-E1A-mediated expression of target genes (e.g. Myc, Cyclin E and E2F)
$K_{\mathrm{A\_EE1}}$	0.8 μM	Hill constant for E2F-E1A-mediated expression of ARF
$K_{\mathrm{C9\_E1E1}}$	0.7 μM	Michaelis constant for E2F-E1A-mediated expression of procaspase-9
$K_{\mathrm{C3\_E1E1}}$	0.5 μM	Michaelis constant for E2F-E1A-mediated expression of procaspase-3
$K_{\mathrm{Af\_E1E1}}$	0.5 μM	Michaelis constant for E2F-E1A-mediated expression of Apaf-1
K_{RpE}	0.2 μM	Michaelis constant for RB_p-E2F-mediated expression of target genes (e.g. Myc, Cyclin E and E2F); it is assumed to be the same as K_{E}
$K_{\mathrm{A\_RpE}}$	1.3 μM	Hill constant for RB_p-E2F-mediated expression of ARF, assumed to be greater than K_{RpE}
$K_{\mathrm{C9\_RpE}}$	1 μM	Michaelis constant for RB_p-E2F-mediated expression of procaspase-9
$K_{\mathrm{C3\_RpE}}$	0.5 μM	Michaelis constant for RB_p-E2F-mediated expression of procaspase-3
$K_{\mathrm{Af\_RpE}}$	1 μM	Michaelis constant for RB_p-E2F-mediated expression of Apaf-1

K_{REE1}	0.2 μM	Michaelis constant for RB-E2F1-E1A-mediated expression of target genes (e.g. Myc, Cyclin E and E2F)
K_{A_REE1}	0.8 μM	Hill constant for RB-E2F1-E1A-mediated expression of ARF
K_{C9_REE1}	0.7 μM	Michaelis constant for RB-E2F1-E1A-mediated expression of procaspase-9
K_{C3_REE1}	0.5 μM	Michaelis constant for RB-E2F1-E1A-mediated expression of procaspase-3
K_{Af_REE1}	0.5 μM	Michaelis constant for RB-E2F1-E1A-mediated expression of Apaf-1
K_{M_p}	0.5 μM	Hill constant for p53-induced expression of MDM2
K_{P_p}	1 μM	Hill constant for p53-induced expression of PTEN, greater than that of MDM2[72]
K_{21_p}	0.3 μM	Hill constant for p53-induced expression of p21
K_{B_p}	0.7 μM	Hill constant for p53-induced activation of Bax
Complex formation or disassociation		
k_{RE}	180 /(μM·h)	Rate constant for RB/E2F association; adapted from Ref. 1
k_{RpE}	60 /(μM·h)	Rate constant for RB_p/E2F1 association, estimated based on k_{RE}
D_{RpE}	30 /h	Rate constant for RB_p-E2F1 disassociation, estimated based on k_{RpE}
k_{EE1}	60 /(μM·h)	Rate constant for E2F/E1A association
D_{EE1}	30 /h	Rate constant for E2F-E1A disassociation
k_{RE1}	180 /(μM·h)	Rate constant for RB-E1A association
k_{REE1}	60 /(μM·h)	Rate constant for the association between RB-E1A and E2F1
D_{REE1}	100 /h	Rate constant for the disassociation of the RB-E2F1-E1A complex
k_{MA}	43 /(μM·h)	Rate constant for MDM2/ARF association
D_{MA}	6 /h	Rate constant for MDM2-ARF disassociation
k_{MpA}	10 /(μM·h)	Rate constant for $MDM2_p$/ARF association
D_{MpA}	24 /h	Rate constant for $MDM2_p$-ARF disassociation
k_{CA}	10 /(μM·h)	Rate constant for Cyt *c*/Apaf-1 association
D_{CA}	2 /h	Rate constant for Cyt *c*-Apaf-1 disassociation
k_{Apop}	10 /(μM·h)	Rate constant for apoptosome formation from Cyt *c*-Apaf-1 dimers

k_{21P} D_{21P}	20 /(μM·h) 1 /h	Rate constant for $p21_p$/procaspase3 association Rate constant for $p21_p$-procaspase3 disassociation
Phosphorylation or dephosphorylation		
k_{p_RB} k_{DP1}	18 /h 3.6 μM/h	Rate constant for RB phosphorylation; adapted from Ref. 1 Rate constant for RB_p dephosphorylation; adapted from Ref. 1
k_{p_RE} k_{DP2}	9 /h 1 μM/h	Rate constant for RB-E2F phosphorylation, assumed to be slower than RB phosphorylation due to additional allosteric transformation Rate constant for RB_p-E2F1 dephosphorylation, assumed to be slower than RB_p dephosphorylation due to additional allosteric transformation
k_{p_RE1}	9 /h	Rate constant for RB-E1A phosphorylation, assumed to be slower than RB phosphorylation due to additional allosteric transformation
k_{p_REE1}	9 /h	Rate constant for RB-E2F1-E1A phosphorylation, assumed to be slower than RB phosphorylation due to additional allosteric transformation
k_{A_S} k_{DP3}	12.9 μM/h 9.6 μM/h	Rate constant for Akt phosphorylation induced by growth factors Rate constant for Akt dephosphorylation
k_{A_P}	30 /h	Rate constant for PTEN-induced Akt dephosphorylation; referring to the dephosphorylation of PIP3 by PTEN[72]
k_{p_M} k_{DP4}	56 /h 12 μM/h	Rate constant for MDM2 phosphorylation mediated by Akt Rate constant for $MDM2_p$ dephosphorylation
k_{p_21} k_{DP5}	20 /h 3 μM/h	Rate constant for p21 phosphorylation mediated by Akt Rate constant for $p21_p$ dephosphorylation
K_{CD} K_{CE}	0.92 μM 0.92 μM	Michaelis constant for cyclin D-mediated phosphorylation; experimentally measured[1] Michaelis constant for cyclin E-mediated phosphorylation, assumed to be the same as K_{CD}[1]
K_{A_S} K_0	1.47% 0.35 μM	Michaelis constant for Akt activation triggered by growth factors Threshold of the total enzyme amount for Akt activation
K_{Akt_M}	0.5 μM	Michaelis constant for Akt-mediated phosphorylation of MDM2[72]
K_{Akt_p21}	0.4 μM	Michaelis constant for Akt-mediated phosphorylation of p21, estimated based on K_{Akt_M}

K_{RBp}	0.01 μM	Michaelis constant for RB_p dephosphorylation; it takes the typical value of the Michaelis constant for dephosphorylation[1]
K_{DRpE}	0.01 μM	Michaelis constant for RB_p-E2F1 dephosphorylation, assumed to be the same as K_{RBp}
K_{Akt}	0.2 μM	Michaelis constant for Akt dephosphorylation
K_{AP}	0.6 μM	Michaelis constant for PTEN-induced Akt dephosphorylation; referring to the Michaelis constant for PTEN-mediated PIP3 dephosphorylation, 0.1~0.5 μM[72]
K_{Mp}	0.081 μM	Michaelis constant for $MDM2_p$ dephosphorylation[72]
K_{p21p}	1 μM	Michaelis constant for $p21_p$ dephosphorylation
Activation of caspase cascade		
k_{Cytc}	0.001 /h	Rate constant for the basal releasing rate of Cyt *c*
k_{C_B}	4 /(μM·h)	Rate constant for Cyt *c* release mediated by Bax oligomers
n_6	2	Hill coefficient for further release of Cyt *c* mediated by caspase-3
k_{C_C3}	40 /h	Rate constant for further release of Cyt *c* induced by caspase-3
K_{C_C3}	0.3 μM	Hill constant for further release of Cyt *c* induced by caspase-3
$Cytc_{free}$	0.14	fraction of free Cyt *c* in mitochondria
$Cytc_{bound}$	0.86	fraction of tightly-bound Cyt *c* in mitochondria
$Cytc_t$	2 μM	Total amount of Cyt *c*, equaling the homeostasis level of Apaf-1[73]
K_{Ct_C3}	0.3 μM	Threshold for caspase-3-induced release of tightly-bound Cyt *c* into the intermembrane space of mitochondria
n_4	4	Hill coefficient for caspase-3-induced solution of Cyt *c*
k_{AP}	10 /(μM·h)	Rate constant for association between apoptosome and procaspase-9
D_{AP}	0.5 /h	Rate constant for disassociation of the A-Pro9 complex
k_{A2P}	10 /(μM·h)	Rate constant for association between A-Pro9 and procaspase-9
k_{A2C}	0.5 /(μM·h)	Rate constant for association between apoptosome and caspase-9
D_{A2C}	1 /h	Rate constant for disassociation of the A-Casp9 holoenzyme
k_{AC9}	11 /h	Rate constant for caspase-3 activation by A-Casp9
K_{AC9}	0.4 μM	Hill constant for caspase-3 activation by A-Casp9
n_5	2	Hill coefficient for caspase-3 activation by A-Casp9

k_{C9} K_{C9} n_5	0.01 /h 1.5 μM 2	Rate constant for caspase-3 activation by caspase-9 Hill constant for caspase-3 activation by caspase-9 Hill coefficient for caspase-3 activation by caspase-9
Protein degradation ($d_{protein} = \ln 2 / T_{1/2} \approx 0.69 / T_{1/2}$)		
d_{Myc}	0.6 /h	Rate constant for Myc degradation; its half-life is about 1 h[1]
d_{CD} d_{CE}	1.3 /h 1.1 /h	Half-life of CycD is 25-30 min[1] Half-life of CycE is about 30 min[1]
d_{E2F}	0.25 /h	Half-life of E2F is 2~3 h[5,6]
d_{RE}	0.04 /h	Half-life of RE is about 12 h[5,6]
d_{RpE}	0.15 /h	Half-life of RB_pE is about 6 h[5,6]
d_{EE1}	0.065 /h	Half-life of E2F-E1A is 10-12 h[6]
d_{REE1}	0.065 /h	Assumed to be the same as d_{EE1}
d_{RB} d_{RBp}	0.06 /h 0.06 /h	Half-life of RB is about 12 h[1] Assumed to be the same as d_{RB}[1]
d_{RE1}	0.01 /h	Half-life of RB-E1A is assumed to be 60 h (E1A protects RB from degradation, which is assumed to be in a similar mechanism to E1A interfering E2F turnover[74])
d_{ARF}	1 /h	Half-life of $p19^{ARF}$ is 6-8 h[75], while that of $p14^{ARF}$ is about 30 min[76]
d_{Mdm2} d_{Mp}	0.5 /h 0.1 /h	Half-life of MDM2 is about 90 min[77] Degradation rate of $MDM2_p$ is about 5-fold slower than that of MDM2[60]
d_{MA} d_{MpA}	0.6 /h	Degradation rate of the MDM2-ARF complex Assumed to be the same as d_{MA}[78]
d_{E1A}	0.5 /h	Half-life of E1A is 20-80 min[79]
d_{PTEN}	0.5 /h	Half-life of PTEN is longer than 8 h[80,81], but PTEN normally undergoes posttranslational modification, which keeps it in an inactive form. The rate constant d_{PTEN} actually represents the decay rate of active PTEN and is much greater than its degradation rate
d_{p53}	3.6 /h	Half-life of p53 is 5-20 min[13,82,83]

k_{M53}	5 /h	Rate constant for MDM2-mediated p53 degradation, assumed to be slower than that mediated by phosphorylated MDM2[13]
K_{M53}	0.5 μM	Assumed to be 5-fold that mediated by $MDM2_p$
k_{Mp53}	18 /h	Rate constant for $MDM2_p$-mediated p53 degradation[84], assumed to be 5-fold d_{p53}
K_{Mp53}	0.1μM	Michaelis constant for MDM2-mediated p53 degradation[84]
d_{21}	1.2 /h	Half-life of p21 in U2OS cells is 30~60 min[85]
d_{21p}	0.4 /h	Half-life of phosphorylated p21 is about 5-6 h[86]
d_{21P}	0.5 /h	Rate constant for degradation of the $p21_p$-procaspase-3 complex; estimated.
k_{C3}	3 /h	Rate constant for the Casp3-mediated cleavage of p21 (or $p21_p$)
K_{C3}	0.3 μM	Hill constant of Casp-3-denpendent cleavage of p21 (or $p21_p$)
d_{Bax}	0.1 /h	Half-life of Bax is about 9-12 h[87]
d_{Cytc}	0.14 /h	Half-life of cytosolic Cyt *c* is about 5 h[88]
d_{Apaf1}	0.7 /h	Under the conditions of apoptosis and caspases activation, the half-life of Apaf-1 is about 60 min[89]
$d_{C\text{-}A}$	3 /h	Rate constant for the decay of functional Cyt *c*-Apaf-1 dimer; its value is relatively great because the aggregation of the dimer into inactive complex is taken into account[18]
d_{Apop}	0.05 /h	Rate constant for disruption of the apoptosome
d_{Pro9}	0.15 /h	Assumed to be comparable with d_{C9}
d_{C9}	0.12 /h	Half-life of Casp9 is about 6 h[90]
d_{Pro3}	0.15 /h	Half-life of Pro3 is about 5.5 h[91]
d_{C3}	0.4 /h	Rate constant for the degradation of Casp3 is 0.3-0.6 according to the half-life of Casp3[92,93]

Methods of parameter estimation

Parameter estimation is based on the following principles:

1) Based on the published theoretical/experimental studies; e.g. the ratio of ARF activated by ectopic E2F to that activated by normal E2F.

2) To ensure a proper timescale for certain reaction process; e.g. the activation time for cyclins and E2F.

3) To ensure a proper steady-state level, we can estimate the range of synthesis rate of a protein based on its experimentally measured degradation rate or half-life.

4) For reversible reactions, such as phosphorylation/dephosphorylation and association/disassociation, only the relative strength of two opposite reactions makes sense in determining the eventual results; so we can estimate the reaction rate in one direction based on that in the opposite direction.

III. SI Appendix Results

1. Effect of E1A on the expression of cyclins

It is obvious that E1A only affects the expression of cyclin E, with the expression of cyclin D unchanged (Fig. S2*A*).

2. Dissecting the biphasic dynamics of E2F activation

The first rapid phase corresponds to E1A-mediated RB blockage and E2F release. First, free RB is completely exhausted before the rapid-to-slow transition point (Fig. S2*B*). At this time point all E2F is free from RB inhibition and all free RB is blocked by E1A. Moreover, the expression rates of E2F's target genes hardly affect the accumulation rate of E2F in the first rapid phase, but affect that in the second slow phase (Fig. S2*C*).

The second slow phase is mainly determined by the transcriptional activity of E2F and E1A/RB-mediated inhibition of E2F degradation. To figure out the role for E2F's transcriptional activity in the second phase, we set several 'restriction points' around the rapid-to-slow transition point (t=3, 3.5, 4, 5, 10 h); i.e., the transcription rates of E2F's target genes are constrained at constant values after the selected time points, equaling their values at 'restriction points' or the saturation levels when E2F is fully activated. We found that the transcription rates determine both the accumulation rate and eventual E2F levels in the second phase (Fig. S2*C*, *left*). Particularly, if the 'restriction point' is set too early, those transcription rates take low values, and thus the E2F level does not rise anymore after the completion of the first phase.

Based on these results, we selected three typical instances, i.e., t=4, 5, 10 h, for further analysis (Fig. S2*C*, *right*). The normalized results indicate that the timescale of the second phase is almost independent of the transcriptional activity of E2F towards its target genes, but is mainly determined by the mechanisms such as degradation inhibition, i.e., E1A/RB-mediated inhibition of E2F degradation.

In brief, the process of E2F activation consists of two phases: the first rapid phase is determined by the E1A-RB interaction, so E2F is rapidly released from RB's inhibition; the second slow phase is mainly determined by the transcriptional activity of E2F and its inhibited degradation mediated by E1A/RB. Specifically, the former dictates the accumulation rate and eventual level of E2F, while the latter determines the timescale of E2F activation in the second phase.

3. Relative strength of Akt versus ARF expression determines p53 levels

As shown in Fig. S2*D*, the data points with the same p53 level lie on lines along the direction of the

positive diagonal of [ARF]-[Akt] plane, with the slope of the lines corresponding to the relative strength of Akt versus ARF. This indicates that the p53 level is determined by the relative strength of Akt versus ARF. The blue region represents the inactive states of p53, where the impact of Akt surpasses that of ARF. The contributions of Akt and ARF are comparable in the green and yellow regions, where p53 remains at moderate levels and most likely induces cell-cycle arrest. The red region is an ARF-dominated region and corresponds to high levels of p53.

4. Dynamics of key components in response to serum starvation and recovery

To advance the understanding of caspase-3 activation when the cell is exposed to serum starvation and recovery, we show the dynamics of key components under various conditions in Figs. S6 and S7. An interpretation in terms of activation of two positive feedback loops in the apoptosis induction module is presented as follows.

The re-addition of 3% serum will lead to upregulation of phosphorylated Akt, which induces a significant increase in phosphorylated p21 ($p21_p$). The majority of procaspase-3 will complex with $p21_p$, and thus only a small amount of caspase-3 can be produced, which fails to trigger the amplification of Cyt *c* release, unless enough Cyt *c* has been released before serum recovery. Thus, T_0 should be so large that Bax and Cyt *c* have accumulated enough. If T approaches T_0 (from below), caspase-3 is not activated due to insufficient procaspase-3, and p21 predominates in the interaction between p21 and caspase-3. If $T>T_0$, Cyt *c* has accumulated to such a level that caspase-3 is continuously produced, which in turn mediates the amplification of Cyt *c* release. Active caspase-3 dominates the double-negative interaction between caspase-3 and p21 and cleaves p21.

For C=8%, much more phosphorylated Akt will be induced after serum recovery, leading to a remarkable decrease in p53 and Bax. Then, the p21 and procaspase-3 levels will drop and elevate markedly, respectively. Thus, a relatively small amount of Cyt *c* can facilitate the conversion from procaspase-3 to caspase-3, indicating a shorter starvation period is sufficient for apoptosis induction. If $T<T_0$, $p21_p$ first complexes with procaspase-3 upon serum re-addition, leading to a sharp decrease in free procaspase-3. Later, p21 drops and procaspase-3 rises. However, Cyt *c* is too little to maintain the accumulation of caspase-3, and the positive feedback involved in Cyt *c* release is not triggered. If $T>T_0$, Cyt *c* and other pro-apoptotic components can accumulate sufficiently to trigger the positive feedback. Nevertheless, it takes a long time for the re-accumulation of procaspase-3; since Bax remains at low levels, the accumulation of Cyt *c*, caspase-9 and A-Casp9 is slowed down. All these render the full activation of caspase-3 markedly delayed.

5. Parameter sensitivity analysis

To check whether the main conclusions drawn in this work hold true generally, we plot the

bifurcation diagram of [caspase-3] for different parameter values when p53 acts in the bistability mode. On each trial, only one parameter is increased or decrease by 10% with respect to its default value, while the others are the same as those in the rightmost panel of Fig. S4*C*. For most parameters, the bifurcation diagrams are similar to Fig. S8*A* (Fig. S9*A*). For 19 out of 119 parameters, the bifurcation diagrams may change qualitatively when the value varies by 10%, as seen in Fig. S9*B*. Those parameters are n_2, n_5, k_{E_E}, d_{E2F}, k_{p53}, k_{p_M}, k_{M_S}, k_{Dp4}, k_{21_p}, K_{21_p}, k_{p_21}, K_{Akt_p21}, k_{C3}, k_{C9_E}, k_{C3_E}, K_{C3}, k_{21P}, K_{AC9}, and d_{C3}, which are mostly related to the regulation of caspase-3, caspase-9, and p21 activities. Nevertheless, only parts of the unstable steady states change markedly, and the stable steady states vary slightly. Accordingly, the T_0-*C* and *F*c-*C* curves are similar to those in Fig. 5*C* (Fig. S9*C*), and the temporal evolution of p53, p21 and caspase-3 levels is also similar to that in Fig. 4 (Fig. S9*D*). Therefore, our main conclusions are insensitive to parameter variations in a limited range.

IV. SI Appendix Figures

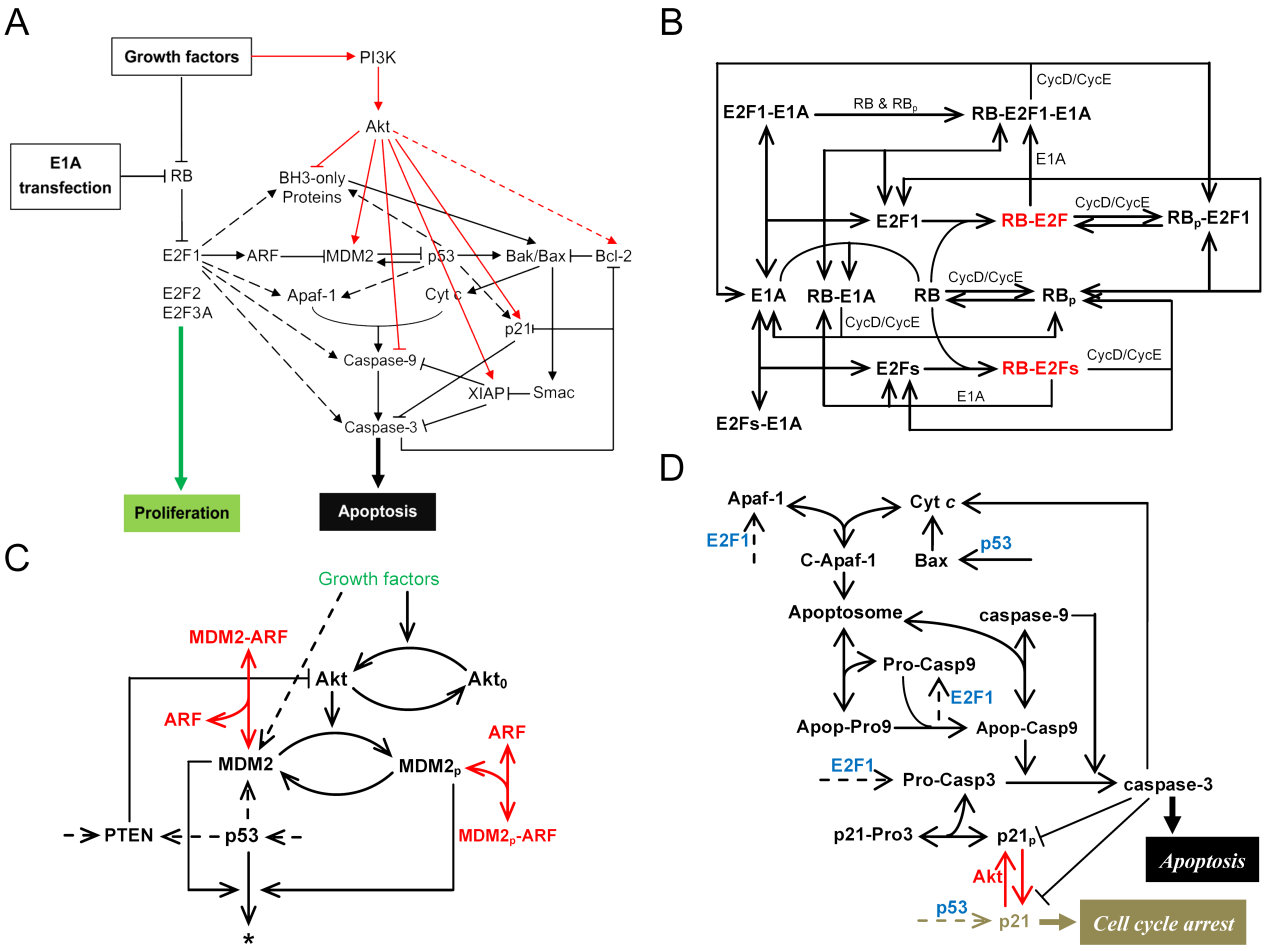

Figure S1: An extended description of cellular signaling involved in tumor suppression.

(*A*) A comprehensive view of Akt-mediated pro-survival pathways. The Akt kinase promotes cell survival through multiple and somewhat redundant pathways. For example, Akt activates Bcl-2 expression through interacting with CREB, promotes the stabilization of XIAP, inhibits the activation of BAD and caspase-9, and facilitates the nuclear export of p21 and nuclear accumulation of MDM2. (*B*) The RB-E2F-cyclin/E1A interaction network. RB normally binds to the transactivation domain (TD) of E2F (including E2F1 and other activator E2Fs), thus blocking its transcriptional activity. The phosphorylation of RB by cyclin D/Cdk4,6 and/or cyclin E/Cdk2 leads to the conformational change and inactivation of RB, resulting in the release of E2Fs rather than E2F1 from RB. Similarly, E1A can release E2Fs from RB. Phosphorylated RB (RB_p) is resistant to binding E1A. E2F can directly interact and form complexes with E1A. (*C*) The p53 activation module. Growth factors in serum not only induce the transcriptional activation of MDM2, but the activation of Akt. Akt phosphorylates MDM2, promoting its nuclear accumulation. As a transcriptional target of p53, MDM2 in turn mediates the ubiquitin-dependent degradation of p53. p53 transactivates PTEN, a tumor

suppressor that dampens Akt activation by dephosphorylating PIP3. The ARF protein interacts with MDM2 and blocks its E3 ligase activity toward p53. (*D*) The module of apoptosis induction mediated by E2F1 and p53. See *Method S1* for details.

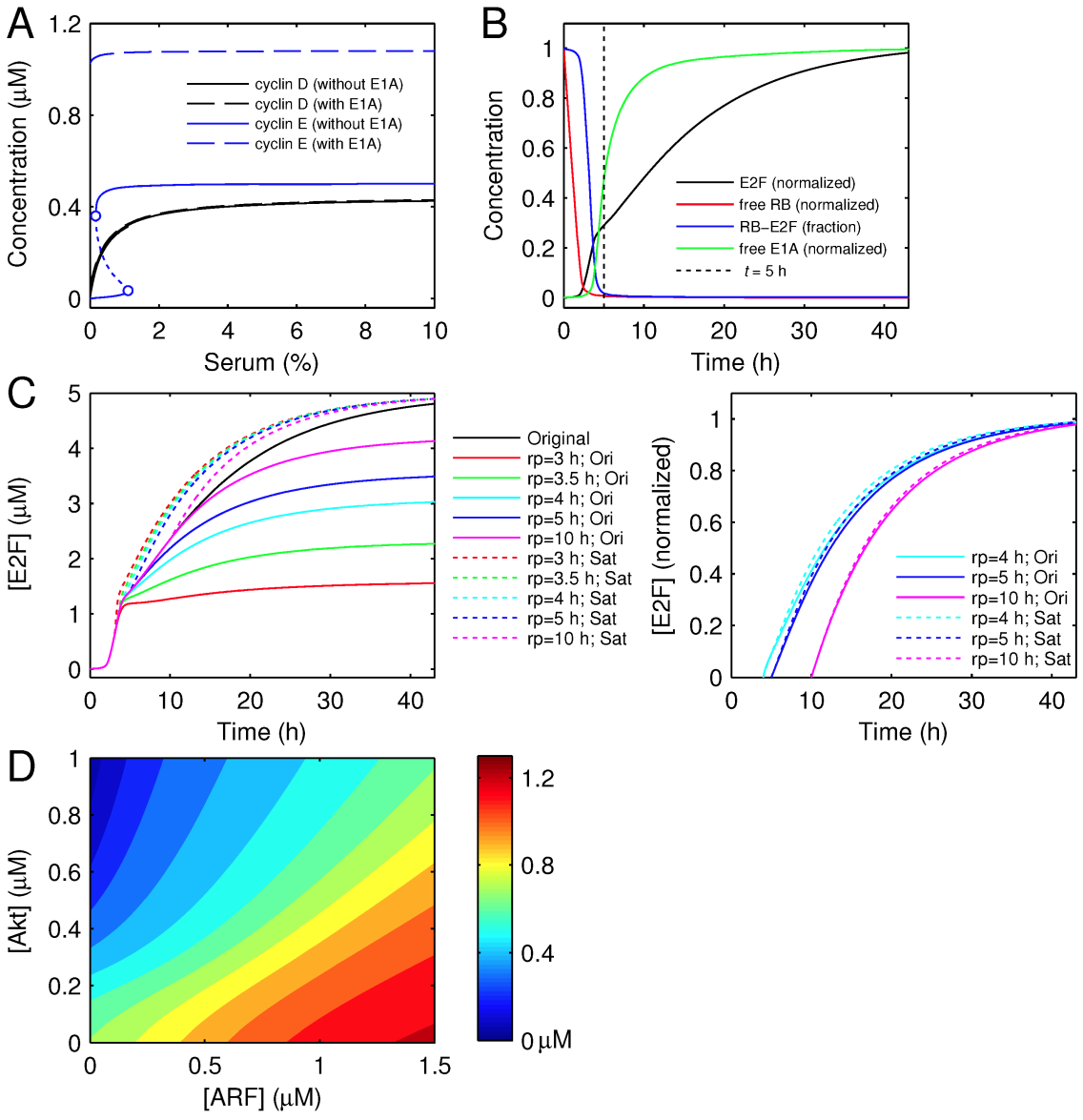

Figure S2: Dynamics of cyclins and effects of ARF and Akt on p53 levels.

(A) Responses of cyclins to serum stimulation with or without E1A expression. The steady-state levels of cyclin D and cyclin E as a function of serum concentration are presented. (***B***) Temporal responses of the concentrations of free RB (normalized), RB-E2F complex (divided by the total E2F level), free E1A (normalized) and active E2F (normalized). The dashed line roughly corresponds to the transition from the rapid to slow phase of E2F activation. (***C***) Dependence of E2F activation on the transcriptional activity of E2F, especially after the rapid-to-slow transition point. We interfere with E2F activation by controlling the rates of

E2F-dependent gene expression; several time points around the transition point are selected for interference (i.e. t=3, 3.5, 4, 5 or 10 h, termed restriction point (rp) hereafter), and the corresponding expression items are set to be constant after these time points, either taking their original values at the restriction points (represented by solid lines) or equaling their saturation levels at t=50 h (dashed lines). The left panel shows the time courses of E2F levels, while the right panel shows the temporal evolution of normalized E2F levels after the restriction points. ***(D)*** Dependence of the steady-state level of p53 on Akt and ARF levels, which are independent inputs. The color box denotes the value of [p53].

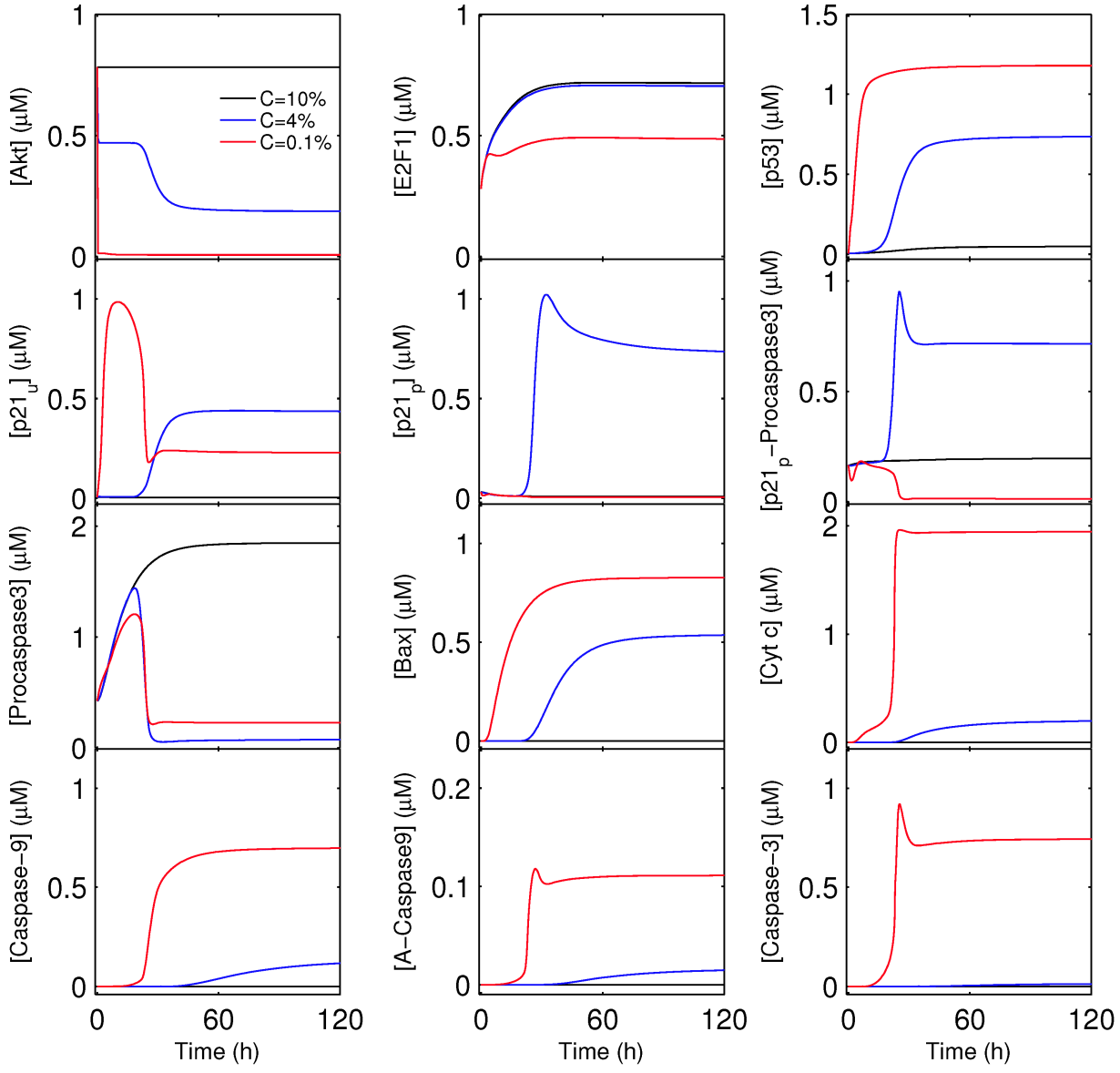

Figure S3：Temporal evolution of key proteins involved in apoptosis induction.

Time courses of proteins for C=0.1%, 4%, or 10%.

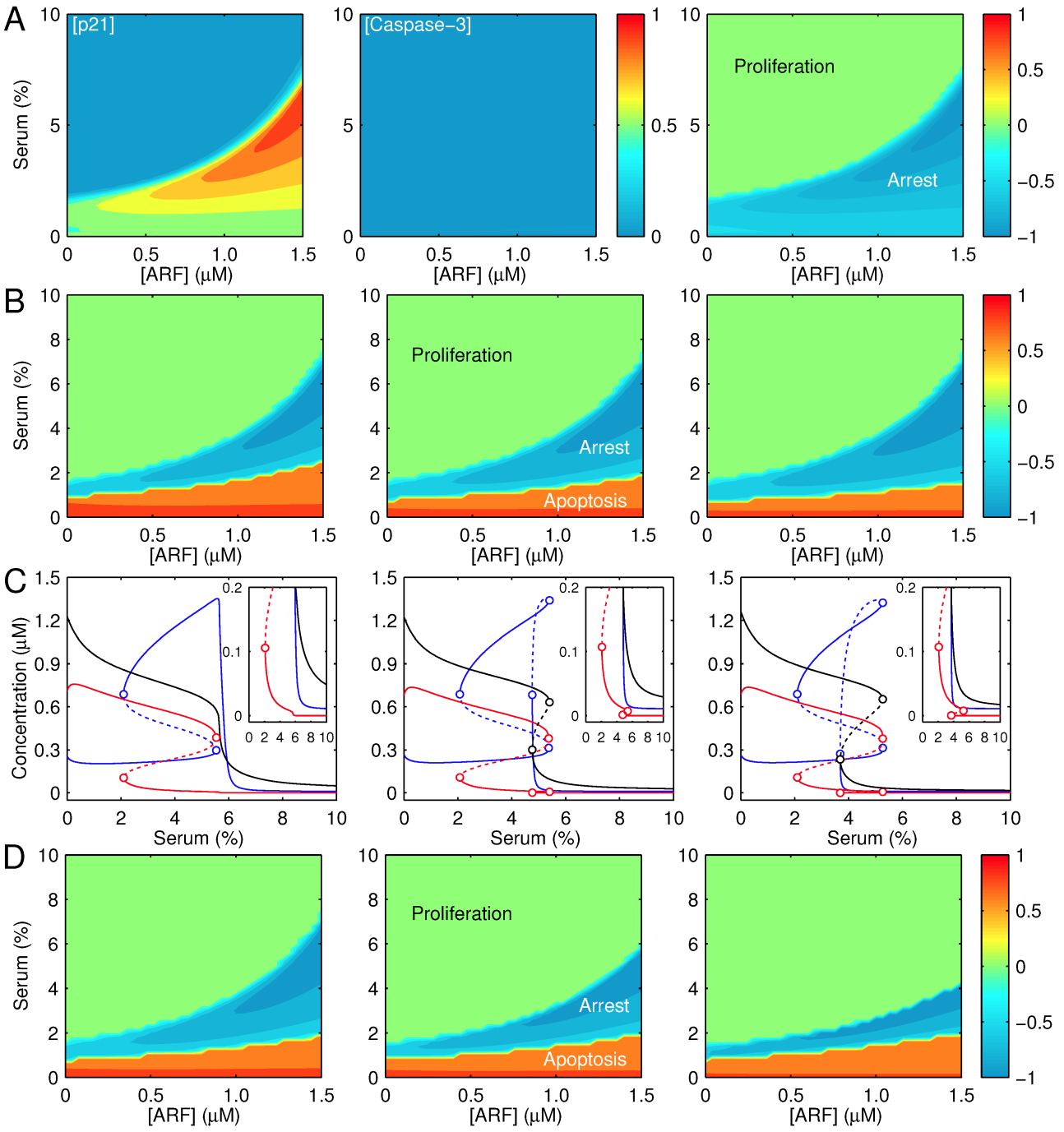

Figure S4: Factors that affect cellular outcome.

(*A*) Protein expression and cell-fate distribution with ARF overexpression. Without E1A expression, the dependence of steady-state levels of p21 (*left*) and caspase-3 (*middle*) on ARF and serum concentrations, which are changed independently. [p21] is normalized by its maximum, while [Caspase-3] is normalized by the maximum of [Caspase-3] in Fig. 3B (i.e., 0.844 μM). Subtracting the p21 level from the caspase-3 level gets a new plot, showing the distribution of cell fate (*right*). (*B*) The inhibitory effect of $p21_p$-Pro3 interaction on apoptosis induction. The same notation as in the *rightmost* plot in panel *A*. Compared with the middle

panel (with the default parameter values), the rate constant for $p21_p$/Pro3 association (k_{21P}) is decreased (*left*) or increased (*right*) by 25%. (***C***) Bifurcation diagrams of the steady-state levels of p21 (*blue*), caspase-3 (*red*) and p53 (*black*) for different modes of p53. For panels from left to right, the bistability domain of p53 expands with different sets of parameter values. ***Left***: k_{M_p}=0.33, K_{M_p}=0.5, n_1=4, k_{MD_S} =0.66, K_{MD_S} =0.45, K_{Mp}=0.081, K_{Akt_M}=0.5, k_{DP4}=12, k_{p_M}=56, k_{DP3}=9.6, K_{Akt}=0.2, k_{C3}=3, k_{REE1}=60, d_{REE1}=0.065; ***middle***: k_{M_p} =0.33, K_{M_p} =0.5, n_1=4, k_{MD_S} =0.66, K_{MD_S} =0.45, K_{Mp} =0.04, K_{Akt_M} =0.5, k_{DP4}=15, k_{p_M} =90, k_{DP3}=9.6, K_{Akt} =0.2, k_{C3}=3, k_{REE1}=100, d_{REE1}=0.08; ***right***: k_{M_p} =0.25, K_{M_p} =0.6, n_1=3, k_{MD_S} =0.77, K_{MD_S}=0.45, K_{Mp} =0.04, K_{Akt_M} =0.5, k_{DP4}=15, k_{p_M} =90, k_{DP3}=9.6, K_{Akt} =0.2, k_{C3}=3, k_{REE1}=80, d_{REE1}=0.08. An enlarged view of each plot is shown in the inset. (***D***) Impact of the kinetic mode of p53 on cellular outcome. The same notation as in panel *B* and the same parameters as in panel *C* are taken here.

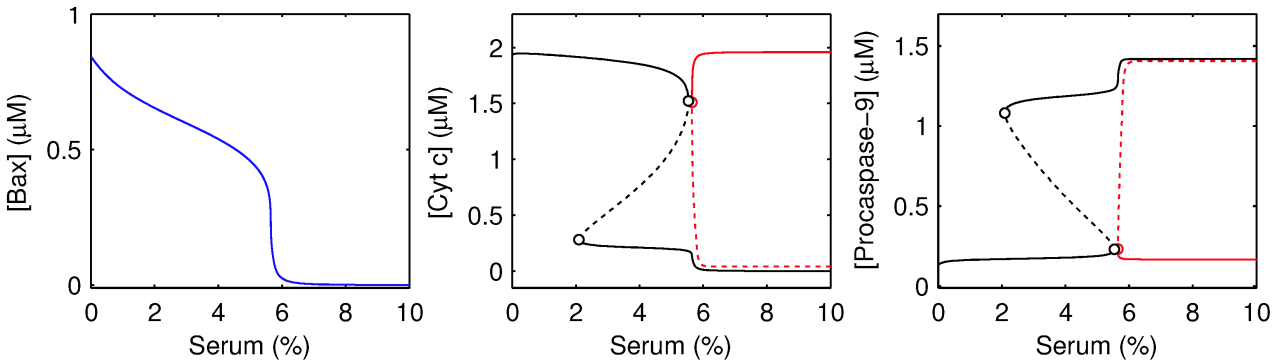

Figure S5: Bifurcation diagrams of steady-state levels of proapoptotic proteins.

The steady-state levels of Bax, Cyt *c* and procaspase-9 are presented. The red curves denote the novel branch. The same parameter values as in Fig. 5*C*.

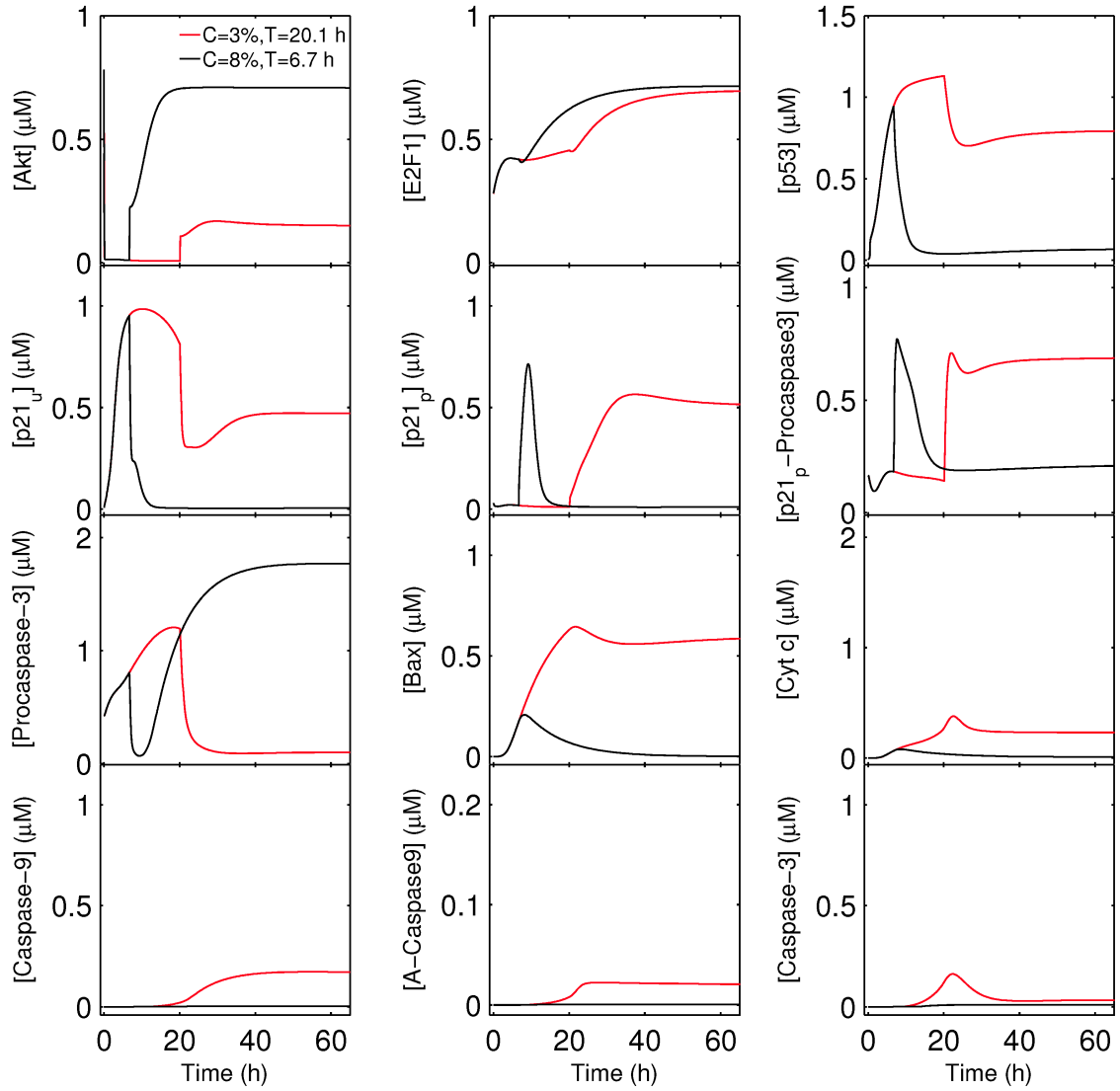

Figure S6: Temporal evolution of key proteins in response to serum starvation and recovery.

The cell is first kept in a serum-free medium for a period of T and then is exposed to 3% (red) or 8% (black) serum. T is smaller than T_0, and the cell undergoes cell-cycle arrest or proliferation. The same parameter values as in Fig. 5*C*. See also the discussion on p. 30.

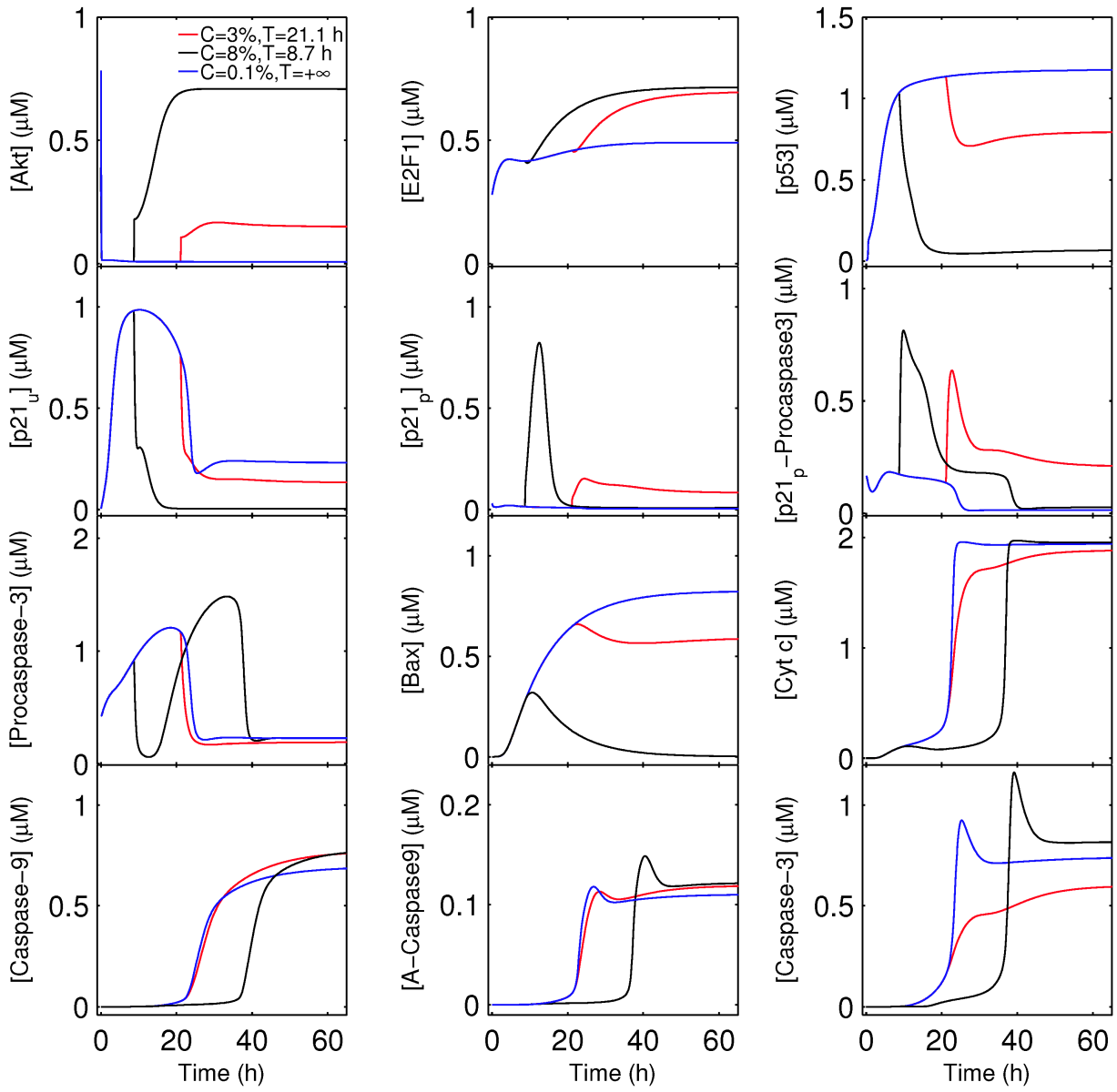

Figure S7: Temporal evolution of key proteins involved in apoptosis induction.

The cell is first kept in a serum-free medium for a period of *T* and then is exposed to 3% (red) or 8% (black) serum. *T* is larger than T_0, and the cell commits apoptosis. For comparison, the cellular response to 0.1% serum is also shown (*blue*). The same parameter values as in Fig. 5*C*. See also the discussion on p. 30.

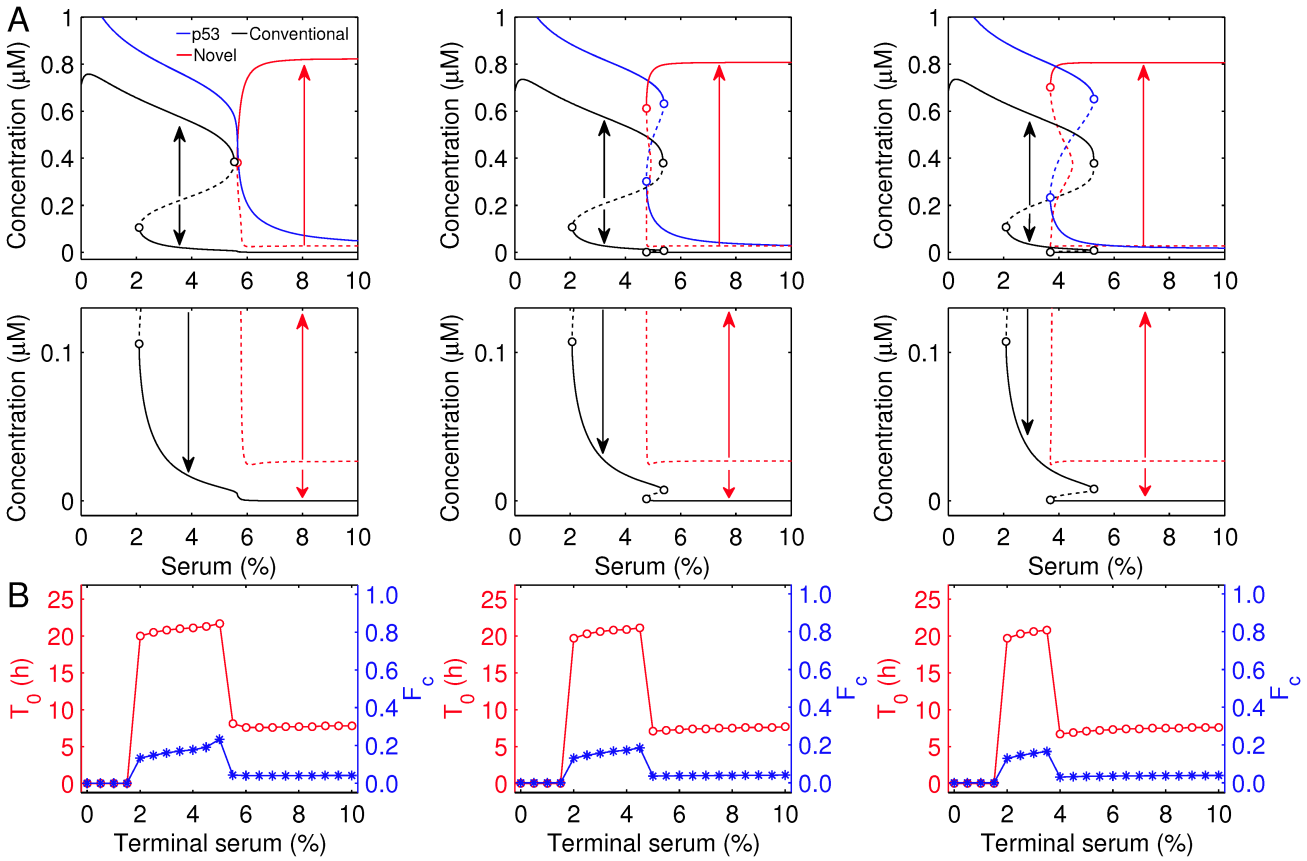

Figure S8: Dependence of the bifurcation diagrams and T_0-C and F_C-C curves on p53 mode.

(***A***) Full bifurcation diagrams of [Caspase-3] and [p53]. From left to right, the p53 mode changes from ultrasensitivity to bistability. The arrows denote the change in [Caspase-3] when its initial value is around an unstable steady-state level. An enlarged view of each plot is shown in the bottom row. (***B***) Dependence of the T_0-C (*red*) and F_C-C (*blue*) curves on the p53 mode. The same parameter values are taken as in Fig. S4*C*.

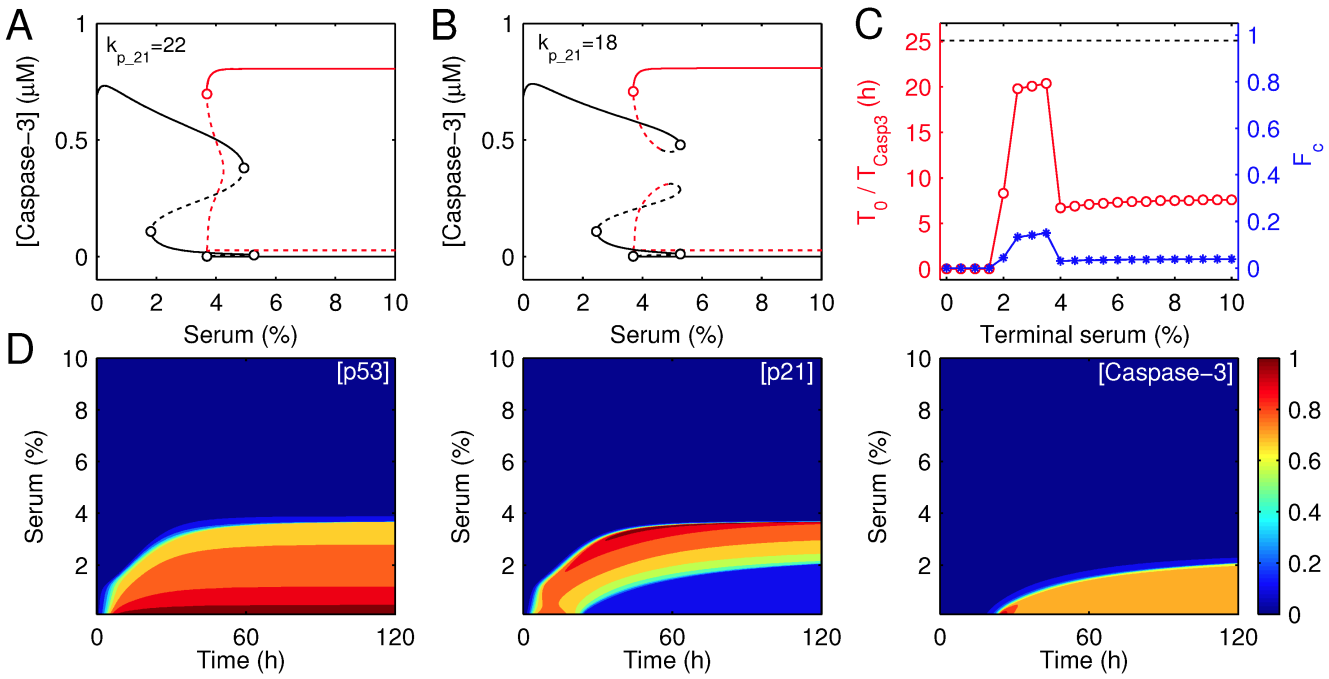

Figure S9: Parameter sensitivity analysis.

The bifurcation diagram of [Caspase-3] for k_{p_21}=22 (***A***) or 18 (***B***); the other parameters are the same as those in the rightmost panel of Fig. S4*C*. (***C***) The T_0-*C* (*red*) and F_C-*C* (*blue*) curves for k_{p_21}=18. The other parameters are the same as those in the rightmost panel of Fig. S4*C*. The same notation and simulation protocol as in Fig. 5*C*. (***D***) Temporal evolution of p53, p21 and caspase-3 levels. The same parameter values as in panel *C*. See also the discussion on p.30-31.

V. References

1 Yao G, Lee TJ, Mori S, Nevins JR, You L. A bistable Rb-E2F switch underlies the restriction point. *Nat Cell Biol* **10**, 476-482 (2008).

2 Ianari A, *et al.* Proapoptotic function of the retinoblastoma tumor suppressor protein. *Cancer Cell* **15**, 184-194 (2009).

3 Seifried LA, *et al.* pRB-E2F1 complexes are resistant to adenovirus E1A-mediated disruption. *J Virol* **82**, 4511-4520 (2008).

4 Cecchini MJ, Dick FA. The biochemical basis of CDK phosphorylation-independent regulation of E2F1 by the retinoblastoma protein. *Biochem J* **434**, 297-308 (2011).

5 Hofmann F, Martelli F, Livingston DM, Wang Z. The retinoblastoma gene product protects E2F-1 from degradation by the ubiquitin-proteasome pathway. *Genes Dev* **10**, 2949-2959 (1996).

6 Hateboer G, Kerkhoven RM, Shvarts A, Bernards R, Beijersbergen RL. Degradation of E2F by the ubiquitin-proteasome pathway: regulation by retinoblastoma family proteins and adenovirus transforming proteins. *Genes Dev* **10**, 2960-2970 (1996).

7 Pelka P, *et al.* Adenovirus E1A directly targets the E2F/DP-1 complex. *J Virol* **85**, 8841-8851 (2011).

8 Green M, Panesar NK, Loewenstein PM. Adenovirus E1A proteins are closely associated with chromatin in productively infected and transformed cells. *Virology* **371**, 1-7 (2008).

9 Heilmann AM, Dyson NJ. Phosphorylation puts the pRb tumor suppressor into shape. *Genes Dev* **26**, 1128-1130 (2012).

10 Ries S, *et al.* Opposing effects of Ras on p53: transcriptional activation of *mdm2* and induction of $p19^{ARF}$. *Cell* **103**, 321-330 (2000).

11 Stambolic V, *et al.* Regulation of PTEN transcription by p53. *Mol Cell* **8**, 317-325 (2001).

12 Manning BD, Cantley LC. AKT/PKB signaling: navigating downstream. *Cell* **129**, 1261-1274 (2007).

13 Zhou BP, *et al. HER-2/neu* induces p53 ubiquitination via Akt-mediated MDM2 phosphorylation. *Nat Cell Biol* **3**, 973-982 (2001).

14 Chipuk JE, *et al.* Direct activation of Bax by p53 mediates mitochondrial membrane permeabilization and apoptosis. *Science* **303**, 1010-1014 (2004).

15 Kuwana T, *et al.* Bid, Bax, and lipids cooperate to form supramolecular openings in the outer mitochondrial membrane. *Cell* **111**, 331-342 (2002).

16 Eskes R, Desagher S, Antonsson B, Martinou JC. Bid induces the oligomerization and

insertion of Bax into the outer mitochondrial membrane. *Mol Cell Biol* **20**, 929-935 (2000).

17 Jürgensmeier JM, *et al.* Bax directly induces release of cytochrome c from isolated mitochondria. *Proc Natl Acad Sci USA* **95**, 4997-5002 (1998).

18 Kim HE, Du F, Fang M, Wang X. Formation of apoptosome is initiated by cytochrome c-induced dATP hydrolysis and subsequent nucleotide exchange on Apaf-1. *Proc Natl Acad Sci USA* **102**, 17545-17550 (2005).

19 Zou H, Li Y, Liu X, Wang X. An APAF-1·cytochrome c multimeric complex is a functional apoptosome that activates procaspase-9. *J Biol Chem* **274**, 11549-11556 (1999).

20 Bratton SB, Salvesen GS. Regulation of the Apaf-1–caspase-9 apoptosome. *J Cell Sci* **123**, 3209-3214 (2010).

21 Malladi S, Challa-Malladi M, Fearnhead HO, Bratton SB. The Apaf-1•procaspase-9 apoptosome complex functions as a proteolytic-based molecular timer. *EMBO J* **28**, 1916-1925 (2009).

22 Nahle Z, *et al.* Direct coupling of the cell cycle and cell death machinery by E2F. *Nat Cell Biol* **4**, 859-864 (2002).

23 Miyashita T, Reed JC. Tumor suppressor p53 is a direct transcriptional activator of the human *bax* gene. *Cell* **80**, 293-299 (1995).

24 Bagci E, Vodovotz Y, Billiar TR, Ermentrout GB, Bahar I. Bistability in apoptosis: roles of Bax, Bcl-2, and mitochondrial permeability transition pores. *Biophys J* **90**, 1546-1559 (2006).

25 Legewie S, Blüthgen N, Herzel H. Mathematical modeling identifies inhibitors of apoptosis as mediators of positive feedback and bistability. *PLoS Comput Biol* **2**, e120 (2006).

26 Spencer SL, Sorger PK. Measuring and modeling apoptosis in single cells. *Cell* **144**, 926-939 (2011).

27 Milojkovic A, *et al.* $p14^{ARF}$ induces apoptosis via an entirely caspase−3−dependent mitochondrial amplification loop. *Int J Cancer* **133**, 2551-2562 (2013).

28 Sherr CJ. Ink4−Arf locus in cancer and aging. *Wiley Interdiscip Rev Dev Biol* **1**, 731-741 (2012).

29 Komori H, Enomoto M, Nakamura M, Iwanaga R, Ohtani K. Distinct E2F−mediated transcriptional program regulates *p14*^{ARF} gene expression. *EMBO J* **24**, 3724-3736 (2005).

30 Iaquinta PJ, Aslanian A, Lees JA. Regulation of the *Arf/p53* tumor surveillance network by E2F. *Cold Spring Harbor Symp Quant Biol* **70**, 309-316 (2005).

31 Aslanian A, Iaquinta PJ, Verona R, Lees JA. Repression of the Arf tumor suppressor by E2F3 is required for normal cell cycle kinetics. *Genes Dev* **18**, 1413-1422 (2004).

32 Jacobs JJ, *et al.* Bmi-1 collaborates with c-Myc in tumorigenesis by inhibiting c-Myc-induced

apoptosis via INK4a/ARF. *Genes Dev* **13**, 2678-2690 (1999).

33 Berk AJ. Recent lessons in gene expression, cell cycle control, and cell biology from adenovirus. *Oncogene* **24**, 7673-7685 (2005).

34 Nevins JR. E2F: A link between the Rb tumor suppressor protein and viral oncoproteins. *Science* **258**, 424-429 (1992).

35 Whyte P, Williamson NM, Harlow E. Cellular targets for transformation by the adenovirus E1A proteins. *Cell* **56**, 67-75 (1989).

36 El-Deiry WS, *et al.* WAF1, a potential mediator of p53 tumor suppression. *Cell* **75**, 817-825 (1993).

37 El-Deiry WS, *et al.* WAF1/CIP1 is induced in p53-mediated G1 arrest and apoptosis. *Cancer Res* **54**, 1169-1174 (1994).

38 Harper JW, Adami GR, Wei N, Keyomarsi K, Elledge SJ. The p21 Cdk-interacting protein Cip1 is a potent inhibitor of G1 cyclin-dependent kinases. *Cell* **75**, 805-816 (1993).

39 Chellappan SP, Hiebert S, Mudryj M, Horowitz JM, Nevins JR. The E2F transcription factor is a cellular target for the RB protein. *Cell* **65**, 1053-1061 (1991).

40 Helin K. Regulation of cell proliferation by the E2F transcription factors. *Curr Opin Genet Dev* **8**, 28-35 (1998).

41 Hermeking H, *et al.* 14-3-3σ is a p53-regulated inhibitor of G2/M progression. *Mol Cell* **1**, 3-11 (1997).

42 Bunz F, *et al.* Requirement for p53 and p21 to sustain G2 arrest after DNA damage. *Science* **282**, 1497-1501 (1998).

43 Chan TA, Hwang PM, Hermeking H, Kinzler KW, Vogelstein B. Cooperative effects of genes controlling the G2/M checkpoint. *Genes Dev* **14**, 1584-1588 (2000).

44 Taylor WR, Stark GR. Regulation of the G2/M transition by p53. *Oncogene* **20,** 1803-1815 (2001).

45 Polager S, Ginsberg D. p53 and E2f: partners in life and death. *Nat Rev Cancer* **9**, 738-748 (2009).

46 Wu X, Levine AJ. p53 and E2F-1 cooperate to mediate apoptosis. *Proc Natl Acad Sci USA* **91**, 3602-3606 (1994).

47 Hershko T, Ginsberg D. Up-regulation of Bcl-2 homology 3 (BH3)-only proteins by E2F1 mediates apoptosis. *J Biol Chem* **279**, 8627-8634 (2004).

48 Moroni MC, *et al.* Apaf-1 is a transcriptional target for E2F and p53. *Nat Cell Biol* **3**, 552-558 (2001).

49 Nakano K, Vousden KH. PUMA, a novel proapoptotic gene, is induced by p53. *Mol Cell* **7**,

683-694 (2001).

50 Miyashita T, *et al.* Tumor suppressor p53 is a regulator of bcl-2 and bax gene expression in vitro and in vivo. *Oncogene* **9**, 1799-1805 (1994).

51 Miyashita T, Harigai M, Hanada M, Reed JC. Identification of a p53-dependent negative response element in the bcl-2 gene. *Cancer Res* **54**, 3131-3135 (1994).

52 Croxton R, Ma Y, Song L, Haura EB, Cress WD. Direct repression of the Mcl-1 promoter by E2F1. *Oncogene* **21**, 1359-1369 (2002).

53 Eischen CM, *et al.* Bcl-2 is an apoptotic target suppressed by both c-Myc and E2F-1. *Oncogene* **20**, 6983-6993 (2001).

54 Cantley LC. The phosphoinositide 3-kinase pathway. *Science* **296**, 1655-1657 (2002).

55 Datta SR, Brunet A, Greenberg ME. Cellular survival: a play in three Akts. *Genes Dev* **13**, 2905-2927 (1999).

56 Zhou BP, *et al.* Cytoplasmic localization of $p21^{Cip1/WAF1}$ by Akt-induced phosphorylation in *HER-2/neu*-overexpressing cells. *Nat Cell Biol* **3**, 245-252 (2001).

57 Child ES, Mann DJ. The intricacies of p21 phosphorylation: protein/protein interactions, subcellular localization and stability. *Cell Cycle* **5**, 1313-1319 (2006).

58 Suzuki A, Tsutomi Y, Akahane K, Araki T, Miura M. Resistance to Fas-mediated apoptosis: activation of Caspase 3 is regulated by cell cycle regulator $p21^{WAF1}$ and IAP gene family ILP. *Oncogene* **17**, 931-939 (1998).

59 Suzuki A, Tsutomi Y, Miura M, Akahane K. Caspase 3 inactivation to suppress Fas-mediated apoptosis: identification of binding domain with p21 and ILP and inactivation machinery by p21. *Oncogene* **18**, 1239-1244 (1999).

60 Ashcroft M, *et al.* Phosphorylation of HDM2 by Akt. *Oncogene* **21**, 1955-1962 (2002).

61 Mayo LD, Donner DB. A phosphatidylinositol 3-kinase/Akt pathway promotes translocation of Mdm2 from the cytoplasm to the nucleus. *Proc Natl Acad Sci USA* **98**, 11598-11603 (2001).

62 Polyak K, Waldman T, He TC, Kinzler KW, Vogelstein B. Genetic determinants of p53-induced apoptosis and growth arrest. *Genes Dev* **10**, 1945-1952 (1996).

63 Gorospe M, *et al.* $p21^{Waf1/Cip1}$ protects against p53-mediated apoptosis of human melanoma cells. *Oncogene* **14**, 929-935 (1997).

64 Hemmati PG, *et al.* Systematic genetic dissection of $p14^{ARF}$-mediated mitochondrial cell death signaling reveals a key role for $p21^{CDKN1}$ and the BH3-only protein Puma/bbc3. *J Mol Med* **88**, 609-622 (2010).

65 Hemmati PG, *et al.* Loss of p21 disrupts $p14^{ARF}$-induced G1 cell cycle arrest but augments

p14^{ARF}-induced apoptosis in human carcinoma cells. *Oncogene* **24**, 4114-4128 (2005).

66 Gervais JL, Seth P, Zhang H. Cleavage of CDK inhibitor p21$^{Cip1/Waf1}$ by caspases is an early event during DNA damage-induced apoptosis. *J Biol Chem* **273**, 19207-19212 (1998).

67 Levkau B, *et al.* Cleavage of p21$^{Cip1/Waf1}$ and p27^{Kip1} mediates apoptosis in endothelial cells through activation of Cdk2: role of a caspase cascade. *Mol Cell* **1**, 553-563 (1998).

68 Chen Q, Gong B, Almasan A. Distinct stages of cytochrome c release from mitochondria: evidence for a feedback amplification loop linking caspase activation to mitochondrial dysfunction in genotoxic stress induced apoptosis. *Cell Death Differ* **7**, 227-233 (2000).

69 Garrido C, *et al.* Mechanisms of cytochrome c release from mitochondria. *Cell Death Differ* **13**, 1423-1433 (2006).

70 Ricci JE, *et al.* Disruption of mitochondrial function during apoptosis is mediated by caspase cleavage of the p75 subunit of complex I of the electron transport chain. *Cell* **117**, 773-786 (2004).

71 Zhu Y, *et al.* Caspase cleavage of cytochrome c1 disrupts mitochondrial function and enhances cytochrome c release. *Cell Res* **22**, 127-141 (2012).

72 Wee KB, Aguda BD. Akt versus p53 in a network of oncogenes and tumor suppressor genes regulating cell survival and death. *Biophys J* **91**, 857-865 (2006).

73 Harrington HA, Ho KL, Ghosh S, Tung KC. Construction and analysis of a modular model of caspase activation in apoptosis. *Theor Biol Med Model* **5**, 26 (2008).

74 Nemajerova A, Talos F, Moll UM, Petrenko O. Rb function is required for E1A-induced S-phase checkpoint activation. *Cell Death Differ* **15**, 1440-1449 (2008).

75 Kuo ML, den Besten W, Bertwistle D, Roussel MF, Sherr CJ. N-terminal polyubiquitination and degradation of the Arf tumor suppressor. *Genes Dev* **18**, 1862-1874 (2004).

76 Chen D, Shan J, Zhu WG, Qin J, Gu W. Transcription-independent ARF regulation in oncogenic stress-mediated p53 responses. *Nature* **464**, 624-627 (2010).

77 Zhang Y, Xiong Y, Yarbrough WG. ARF promotes MDM2 degradation and stabilizes p53: ARF-INK4a locus deletion impairs both the Rb and p53 tumor suppression pathways. *Cell* **92**, 725-734 (1998).

78 Xirodimas D, Saville MK, Edling C, Lane DP, Lain S. Different effects of p14^{ARF} on the levels of ubiquitinated p53 and Mdm2 *in vivo*. *Oncogene* **20**, 4972-4983 (2001).

79 Frisch SM, Mymryk JS. Adenovirus-5 E1A: paradox and paradigm. *Nat Rev Mol Cell Biol* **3**, 441-452 (2002).

80 Wu X, *et al.* Evidence for regulation of the PTEN tumor suppressor by a membrane-localized multi-PDZ domain containing scaffold protein MAGI-2. *Proc Natl Acad Sci USA* **97**,

4233-4238 (2000).

81 Xu D, Yao Y, Jiang X, Lu L, Dai W. Regulation of PTEN stability and activity by Plk3. *J Biol Chem* **285**, 39935-39942 (2010).

82 Giaccia AJ, Kastan MB. The complexity of p53 modulation: emerging patterns from divergent signals. *Genes Dev* **12**, 2973-2983 (1998).

83 Sherr CJ, Weber JD. The ARF/p53 pathway. *Curr Opin Genet Dev* **10**, 94-99 (2000).

84 Ma L, *et al.* A plausible model for the digital response of p53 to DNA damage. *Proc Natl Acad Sci USA* **102**, 14266-14271 (2005).

85 Maki CG, Howley PM. Ubiquitination of p53 and p21 is differentially affected by ionizing and UV radiation. *Mol Cell Biol* **17**, 355-363 (1997).

86 Li Y, Dowbenko D, Lasky LA. AKT/PKB phosphorylation of $p21^{Cip/WAF1}$ enhances protein stability of $p21^{Cip/WAF1}$ and promotes cell survival. *J Biol Chem* **277**, 11352-11361 (2002).

87 Xin M, Deng X. Nicotine inactivation of the proapoptotic function of Bax through phosphorylation. *J Biol Chem* **280**, 10781-10789 (2005).

88 Bobba A, *et al.* Early release and subsequent caspase-mediated degradation of cytochrome c in apoptotic cerebellar granule cells. *FEBS Lett* **457**, 126-130 (1999).

89 Lauber K, *et al.* The adapter protein apoptotic protease-activating factor-1 (Apaf-1) is proteolytically processed during apoptosis. *J Biol Chem* **276**, 29772-29781 (2001).

90 Hao Y, *et al.* Apollon ubiquitinates SMAC and caspase-9, and has an essential cytoprotection function. *Nat Cell Biol* **6**, 849-860 (2004).

91 Tan M, *et al.* SAG/ROC-SCF β-TrCP E3 ubiquitin ligase promotes pro-caspase-3 degradation as a mechanism of apoptosis protection. *Neoplasia* **8**, 1042-1054 (2006).

92 Du JQ, *et al.* Isoquinoline-1, 3, 4-trione derivatives inactivate caspase-3 by generation of reactive oxygen species. *J Biol Chem* **283**, 30205-30215 (2008).

93 Kumar MS, *et al.* Designing a promotor for a novel target site identified in caspases for initiating apoptosis in cancer cells. *Information and Communication Technologies*. 62-67 (Springer, 2010).